



ARTICLE

Optimal Fuzzy Tracking Synthesis for Nonlinear Discrete-Time Descriptor Systems with T-S Fuzzy Modeling Approach

Yi-Chen Lee¹, Yann-Horng Lin², Wen-Jer Chang^{2,*}, Muhammad Shamrooz Aslam^{3,*} and Zi-Yao Lin²

¹Department of Information Management, National Dong Hwa University, Hualien, 974, Taiwan

²Department of Marine Engineering, National Taiwan Ocean University, Keelung, 202, Taiwan

³Artificial Intelligence Research Institute, China University of Mining and Technology, Xuzhou, 2211106, China

*Corresponding Authors: Wen-Jer Chang. Email: wjchang@mail.ntou.edu.tw;
Muhammad Shamrooz Aslam. Email: shamroz_aslam@cumt.edu.cn

Received: 21 February 2025; Accepted: 17 April 2025; Published: 30 May 2025

ABSTRACT: An optimal fuzzy tracking synthesis for nonlinear discrete-time descriptor systems is discussed through the Parallel Distributed Compensation (PDC) approach and the Proportional-Difference (P-D) feedback framework. Based on the Takagi-Sugeno Fuzzy Descriptor Model (T-SFDM), a nonlinear discrete-time descriptor system is represented as several linear fuzzy subsystems, which facilitates the linear P-D feedback technique and streamlines the fuzzy controller design process. Leveraging the P-D feedback fuzzy controller, the closed-loop T-SFDM can be transformed into a standard system that guarantees non-impulsiveness and causality for the nonlinear discrete-time descriptor system. In view of the disturbance problems, a passive performance constraint is incorporated into the fuzzy tracking synthesis to achieve dissipativity of disturbance energy. To achieve a better balance between state and control responses, the H_2 performance requirement is considered and a minimization constraint is applied to optimize the H_2 index. It is observed that there is a lack of research focusing on both disturbance and control input issues in nonlinear descriptor systems. Extending the Lyapunov theory, a stability analysis method is proposed for the tracking purpose with the combination of the free-weighting matrix to relax the analysis process while complying multiple performance constraints. Finally, two simulation examples are presented to demonstrate the feasibility and applicability of the proposed approach in practical control scenarios for nonlinear descriptor systems.

KEYWORDS: Nonlinear descriptor system; takagi-sugeno fuzzy model; H_2 performance; passive performance; robustness; fuzzy tracking synthesis

1 Introduction

Over the past few decades, the control problem of nonlinear systems has been extensively addressed [1]. In practical systems, there are often inherent nonlinearities that must be considered to more precisely describe the dynamics of control systems. Additionally, systems in descriptor form have been shown to provide a powerful tool for enhancing the completeness in describing practical control systems [2,3]. It is worth noting that not only is the implicit relation included to represent the interrelations in many systems, but there also exist purely static relations featuring identity correlations among different dynamic variables. Because of this reason, the description of descriptor systems includes both differential and algebraic equations, thus being referred to as differential-algebraic systems [4]. Descriptor systems can also be applied to situations involving singularities, singular perturbations, and noncausalities. Notably, singular systems have been widely discussed due to their use in various control scenarios, such as acceleration and its



derivative, autonomous ships, as well as bio-economic systems [5–7]. However, the algebraic constraints in descriptor systems also lead to the issue of infinite poles and impulse behaviors [8,9], as the static relationships must be satisfied at a given instant. Taking advantage of large-scale systems, the control and analysis of nonlinear descriptor systems have attracted significant attention [10]. Nevertheless, the nonlinearities and algebraic constraints still pose formidable challenges to the development of controller design approaches.

Consequently, ensuring the absence of impulse modes has emerged as a critical consideration in the controller design of nonlinear descriptor systems. To address this issue, a proportional and derivative feedback concept has been introduced to transform the closed-loop system into a regular system [11,12]. That is, the feedback signal guarantees non-impulsiveness and causality for the system. For discrete-time systems, this concept is referred to as Proportional-Difference (P-D) feedback [13]. Due to the nonlinearities, the development of controller design approaches for nonlinear descriptor systems is confronted with significant challenges and complexities. Over the past decades, the Takagi-Sugeno Fuzzy Model (T-SFM) has proven to be a powerful tool for tackling the control problem of nonlinear systems [14]. By characterizing a nonlinear system as several linear subsystems, the controller design problem is efficiently reduced to a linear problem. In other words, the linear P-D feedback technique can be utilized in the control problem of nonlinear descriptor systems. Leveraging the T-SFM and Parallel Distributed Compensation (PDC) framework, some researchers have successfully developed fuzzy P-D controllers to stabilize the nonlinear descriptor systems [15,16]. Moreover, some simulations have been implemented to explore practical applications [17–18]. Nevertheless, disturbance and uncertainty issues must be resolved to enhance the reliability of the control approach. The trade-off between convergence rate and control cost should also be considered while meeting practical control requirements.

In most industrial systems, external disturbances, such as power quality disturbances for generators [19], road roughness for electric power steering systems [20], and winds and waves for ships [21], are inevitable and persistent factors. In view of disturbance problem, many researchers have contributed to the development of anti-disturbance control approaches for nonlinear descriptor systems [22,23]. From the energy perspective, passive performance has been introduced to achieve the dissipativity of external energy [24]. A system can be called a dissipative system because the energy dissipated inside is less than the energy supplied by the external source [24,25]. Therefore, several researchers have successfully extended the concept of dissipativity to the disturbance problem, where disturbance energy is regarded as external energy [25,26]. In [25,27], the researchers have also presented the energy supply function such that the system consumption energy is always greater than the external energy to achieve this dissipativity. Passivity theory has long been recognized as an effective tool for the analysis of electrical networks and nonlinear systems. It is worth noting that the passive performance constraint provides a general framework for various considerations, including H_∞ , strictly input passivity, and other related forms, depending on the setting of the energy supply function. Moreover, uncertainties pose a significant challenge in enhancing control performance for practical applications [28,29]. Fuzzy theory is widely recognized as an effective approach to addressing uncertainties in daily life and engineering systems [30]. Nevertheless, the T-SFM constructed for actual nonlinear systems may involve modeling errors [31]. Based on the T-SFM, some researchers have improved the identification and control issues using adaptive control under system uncertainties [32]. Extending the control issue, some researchers have also solved the controller design problem for uncertain nonlinear descriptor systems [33]. By employing proportional and derivative feedback techniques, fuzzy controllers have also been successfully developed to handle uncertainty and disturbance issues [34]. However, the development of tracking controllers using the P-D fuzzy control scheme for discrete-time descriptor systems remains an unresolved challenge.

More importantly, the control effort required to ensure both the passive constraint and robustness may increase significantly. For specific objectives such as trajectory tracking, the responses of the controlled variables could become excessively drastic, which is not suitable for practical control applications. Furthermore, the control cost could potentially exceed practical requirements, leading to inefficiency. The H_2 performance index has been introduced to evaluate the energy of state and input [35]. It has also been recognized as a powerful performance metric in the control of autonomous vehicles [36]. The application of the H_2 performance index is often accompanied by a minimization constraint, which aims to optimize the energy associated with the index. Nowadays, some researchers have successfully extended the H_2/H_∞ constraint to the fuzzy controller design for the tracking problem in nonlinear systems under the T-S fuzzy model framework [37]. Based on the descriptor form, the T-S Fuzzy Descriptor Model (T-SFDM) based fuzzy controller design have been investigated with disturbance and uncertainty problems in several papers [38]. Considering the control efficiency while affected by the external disturbances, an input shaping approach has been developed under H_∞ performance for the fuzzy tracking control problem [39]. Nonetheless, there is lack of existing papers discussing the multiple-performance-constrained problem for discrete-time nonlinear descriptor systems, even for their tracking issue. However, the difficulty of the tracking controller design problem subject to multiple constraints increases significantly due to the nonlinearities and descriptor form. By leveraging the linear representation of subsystems in T-SFDM, the complexity of the design process can be effectively reduced.

The reason outlined above motivated this research to propose a fuzzy tracking synthesis for discrete-time nonlinear descriptor systems that satisfies multiple performance criteria, including robustness, passivity, and optimal H_2 . First, the T-SFDM is established for a class of nonlinear descriptor systems. Considering the existence of modeling errors, the T-SFDM is also constructed for the target trajectory with uncertain factors. Next, the T-S Fuzzy Descriptor Error Model (T-SFDEM) is derived by subtracting the target model from the T-SFDM. With the same premise as the T-SFDEM, a PDC-based fuzzy controller is developed using the P-D error feedback signals. For the closed-loop T-SFDEM, a definition is provided to examine the regularity and causality. Additionally, the constraints of robust control, passive performance, and H_2 performance are introduced separately. Based on the multiple performance constraints and Lyapunov theory, a stability criterion is proposed to ensure the stability of the error dynamics and achieve the trajectory tracking objective. It is worth noting that the free-weighting matrix technique is integrated into the analysis process to further reduce the conservativeness caused by the multiple constraints, particularly the minimization of H_2 performance. Consequently, the stability criteria are derived into the Linear Matrix Inequality (LMI) problem, enabling efficient solutions via computational tools. Finally, two simulation examples, including a nonlinear DC-motor system and a ship steering system, are provided to demonstrate the feasibility and effectiveness of the proposed P-D fuzzy tracking controller.

This paper is organized as follows. In [Section 2](#), the T-SFDM and the corresponding T-SFDEM are obtained. In [Section 3](#), a P-D feedback fuzzy tracking synthesis is proposed for the tracking purpose. In [Section 4](#), two simulation examples, including a nonlinear DC motor system and a ship steering system, are provided. Based on the results, some conclusions are given in [Section 5](#).

2 System Description and Problem Statement

In this section, the T-SFDMs of nonlinear descriptor systems and target trajectory are respectively established. Then, the T-SFDEM is obtained from two T-SFDMs. According to the PDC design concept, the P-D fuzzy tracking controller is presented. Some definitions and lemmas related to multiple performance requirements are also introduced. First, the T-SFDM is presented as follows.

Model Rules α :

If $\vartheta_1(k)$ is $\phi_{\alpha 1}$ and $\vartheta_2(k)$ is $\phi_{\alpha 2}$ and... and $\vartheta_\ell(k)$ is $\phi_{\alpha \ell}$, then

$$\begin{cases} \widehat{\mathfrak{T}}_\alpha(k) x(k+1) = \widehat{\mathbf{A}}_\alpha(k) x(k) + \widehat{\mathbf{B}}_\alpha(k) u(k) + \mathbf{W}_\alpha w(k) \\ y(k) = \mathbf{C}_\alpha x(k) + \mathbf{V}_\alpha w(k) \end{cases} \quad (1)$$

where model matrices $\widehat{\mathfrak{T}}_\alpha(k) = \mathfrak{T}_\alpha + \Delta\mathfrak{T}_\alpha(k)$, $\widehat{\mathbf{A}}_\alpha(k) = \mathbf{A}_\alpha + \Delta\mathbf{A}_\alpha(k)$, $\widehat{\mathbf{B}}_\alpha(k) = \mathbf{B}_\alpha + \Delta\mathbf{B}_\alpha(k)$ are constructed with the time-varying uncertainties, $x(k) \in R^s$, $u(k) \in R^i$, $y(k) \in R^o$ and $w(k) \in R^d$ respectively are the system's state, input, output and disturbance vectors, $\vartheta_1(k)$ to $\vartheta_\ell(k)$ are the premise variables, $\phi_{\alpha 1}$ to $\phi_{\alpha \ell}$ are the fuzzy sets, $\alpha = 1, 2, \dots, \tau$ and $\varsigma = 1, 2, \dots, \ell$ are the numbers of premise variables and fuzzy rules. Note that the matrix \mathfrak{T}_α , with or without full rank, can be used to describe the singular and typical systems in descriptor form.

In the T-SFDM (1), $\Delta\mathfrak{T}_\alpha(k)$, $\Delta\mathbf{A}_\alpha(k)$ and $\Delta\mathbf{B}_\alpha(k)$ represent the time-varying uncertain factors that may arise from modeling parameter errors and other relevant factors. Then, these matrices are further decomposed into the following structure.

$$\Delta\mathfrak{T}_\alpha(k) = \mathbf{H}_\alpha \Delta_\alpha(k) \mathbf{R}_{\mathfrak{T}_\alpha}, \Delta\mathbf{A}_\alpha(k) = \mathbf{H}_\alpha \Delta_\alpha(k) \mathbf{R}_{\mathbf{A}_\alpha}, \text{ and } \Delta\mathbf{B}_\alpha(k) = \mathbf{H}_\alpha \Delta_\alpha(k) \mathbf{R}_{\mathbf{B}_\alpha} \quad (2)$$

where $\Delta_\alpha(k)$ denotes the time-varying uncertain item, \mathbf{H}_α , $\mathbf{R}_{\mathfrak{T}_\alpha}$, $\mathbf{R}_{\mathbf{A}_\alpha}$ and $\mathbf{R}_{\mathbf{B}_\alpha}$ denote the structure of uncertainties, with appropriate dimensions.

Then, the following overall T-SFDM is obtained by blending with all fuzzy subsystems in (1) with membership functions.

$$\begin{cases} \sum_{\alpha=1}^{\tau} \Phi_\alpha(\vartheta(k)) \left\{ \widehat{\mathfrak{T}}_\alpha(k) x(k+1) \right\} = \sum_{\alpha=1}^{\tau} \Phi_\alpha(\vartheta(k)) \left\{ \widehat{\mathbf{A}}_\alpha(k) x(k) + \widehat{\mathbf{B}}_\alpha(k) u(k) + \mathbf{W}_\alpha w(k) \right\} \\ y(k) = \sum_{\alpha=1}^{\tau} \Phi_\alpha(\vartheta(k)) \left\{ \mathbf{C}_\alpha x(k) + \mathbf{V}_\alpha w(k) \right\} \end{cases} \quad (3)$$

where $\Phi_\alpha(\vartheta(k)) = \prod_{\varsigma=1}^{\ell} \phi_{\alpha \varsigma}(\vartheta_\varsigma(k)) / \sum_{\alpha=1}^{\tau} \prod_{\varsigma=1}^{\ell} \phi_{\alpha \varsigma}(\vartheta_\varsigma(k))$, which satisfies the situation $\sum_{\alpha=1}^{\tau} \Phi_\alpha(\vartheta(k)) > 0$ and $\Phi_\alpha(\vartheta(k)) \geq 0$, $\varsigma = 1, 2, \dots, \ell$ is the number of premise variables. To simplify the expressions in this research, the time-varying terms involving premise variables and uncertainties, denoted as $\widehat{\mathfrak{T}}_\alpha(k)$, $\widehat{\mathbf{A}}_\alpha(k)$, $\widehat{\mathbf{B}}_\alpha(k)$, $\Phi_\alpha(\vartheta(k))$, are reduced to \mathfrak{T}_α , \mathbf{A}_α , \mathbf{B}_α and Φ_α throughout the remainder of this paper.

For the tracking purpose, the T-SFDM is also constructed as follows, with consideration of the parameter uncertainty caused by modeling errors, similar to the process described in Eqs. (1)–(3).

$$\begin{cases} \sum_{\alpha=1}^{\tau} \Phi_\alpha \left\{ \widehat{\mathfrak{T}}_\alpha x_d(k+1) \right\} = \sum_{\alpha=1}^{\tau} \Phi_\alpha \left\{ \widehat{\mathbf{A}}_\alpha x_d(k) \right\} \\ y_d(k) = \sum_{\alpha=1}^{\tau} \Phi_\alpha \left\{ \mathbf{C}_\alpha x_d(k) \right\} \end{cases} \quad (4)$$

where $x_d(k)$ and $y_d(k)$ denote the desired state and output trajectories.

Then, the tracking T-SFDEM is obtained as follows from (3) and (4).

$$\begin{cases} \sum_{\alpha=1}^{\tau} \Phi_{\alpha} \left\{ \widehat{\mathfrak{T}}_{\alpha} e_x(k+1) \right\} = \sum_{\alpha=1}^{\tau} \Phi_{\alpha} \left\{ \widehat{\mathbf{A}}_{\alpha} e_x(k) + \widehat{\mathbf{B}}_{\alpha} u(k) + \mathbf{W}_{\alpha} w(k) \right\} \\ e_y(k) = \sum_{\alpha=1}^{\tau} \Phi_{\alpha} \left\{ \mathbf{C}_{\alpha} e_x(k) + \mathbf{V}_{\alpha} w(k) \right\} \end{cases} \quad (5)$$

where $e_x(k) = x(k) - x_d(k)$ and $e_y(k) = y(k) - y_d(k)$ are the tracking errors of the system's states and outputs.

According to the T-SFDEM (5), the following P-D error feedback fuzzy controller is developed by the PDC framework to complete the tracking task.

$$u(k) = \sum_{\alpha=1}^{\tau} \Phi_{\alpha} \left\{ \mathbf{T}_{\alpha}^p e_x(k) - \mathbf{T}_{\alpha}^d e_x(k+1) \right\} \quad (6)$$

where \mathbf{T}_{α}^p and \mathbf{T}_{α}^d are the gains for the proportional and difference feedback terms. It is observed that Φ_{α} of the premise part is designed in the same way as the T-SFDEM (5) to comply with the PDC concept. To make the application of P-D feedback concept more meaningful, Remark 1 is presented to illustrate the use of feedback signals.

Remark 1. Building on the results of research on linear discrete-time descriptor systems, including but not limited to [40,41], $k + 1$ is considered the current time instant, which can be derived from the previous time instant k when there is a design of the state observer. However, observer design is not the primary focus of this research; the main discussion is centered on the design of the multi-performance P-D fuzzy tracking controller. For this reason, all states of the control systems are assumed to be available for the implementation of the P-D feedback technique.

Therefore, the following closed-loop T-SFDEM is obtained by substituting the P-D fuzzy tracking controller (6) into T-SFDEM (5).

$$\begin{cases} \sum_{\alpha=1}^{\tau} \sum_{\beta=1}^{\tau} \Phi_{\alpha} \Phi_{\beta} \left\{ \widehat{\mathbf{Q}}_{\alpha\beta}^d e_x(k+1) \right\} = \sum_{\alpha=1}^{\tau} \sum_{\beta=1}^{\tau} \Phi_{\alpha} \Phi_{\beta} \left\{ \widehat{\mathbf{Q}}_{\alpha\beta}^p e_x(k) + \mathbf{W}_{\alpha} w(k) \right\} \\ e_y(k) = \sum_{\alpha=1}^{\tau} \Phi_{\alpha} \left\{ \mathbf{C}_{\alpha} e_x(k) + \mathbf{V}_{\alpha} w(k) \right\} \end{cases} \quad (7)$$

where $\widehat{\mathbf{Q}}_{\alpha\beta}^d = \widehat{\mathfrak{T}}_{\alpha} + \widehat{\mathbf{B}}_{\alpha} \mathbf{T}_{\beta}^d$ and $\widehat{\mathbf{Q}}_{\alpha\beta}^p = \widehat{\mathbf{A}}_{\alpha} + \widehat{\mathbf{B}}_{\alpha} \mathbf{T}_{\beta}^p$ are the closed-loop matrices.

Conducting an examination of regularity and causality, Definition 1 is presented for the T-SFDEM.

Definition 1. If the following situations are satisfied, the regularity and causality of the closed-loop T-SFDEM (7) are guaranteed, and the system's responses will be impulsive-free.

- (a) The system is said to be regular when $\det \left(z \widehat{\mathfrak{T}}_{\alpha} - \widehat{\mathbf{A}}_{\alpha} \right) \neq 0$.
- (b) The system is said to be causal when $\deg \left(\det \left(z \widehat{\mathfrak{T}}_{\alpha} - \widehat{\mathbf{A}}_{\alpha} \right) \right) = \text{rank} \left(\widehat{\mathfrak{T}}_{\alpha} \right)$.

where $\det(\cdot)$ and $\deg(\cdot)$ denote the determinant and its degree.

It is obvious that the two situations are certainly ensured for the typical system, where $\widehat{\mathfrak{T}}_{\alpha}$ is of full rank. With the P-D fuzzy tracking controller (6), the conditions in Definition 1 can also be guaranteed for the closed-loop T-SFDEM (7) even when $\widehat{\mathfrak{T}}_{\alpha}$ is a singular matrix. The P-D feedback technique can effectively

transform the singular system into a regular form by ensuring that the matrix $\widehat{\mathbf{Q}}_{\alpha\beta}^d$ is of full rank. Aiming to address the uncertainty problems, an inequality for robust control is introduced in Lemma 1.

Lemma 1. [42]. For a scalar ω , the following result is satisfied by assigning the constant matrices \mathbf{H} and \mathbf{R} of appropriate dimension.

$$\mathbf{H}\Delta(k)\mathbf{R} + \mathbf{R}^T\Delta^T(k)\mathbf{H}^T \leq \omega\mathbf{H}\mathbf{H}^T + \omega^{-1}\mathbf{R}^T\mathbf{R} \quad (8)$$

where time-varying uncertain term $\Delta(k)$ satisfies $\Delta(k)\Delta^T(k) \leq \mathbf{I}$.

In the context of the energy concept, the following passive performance constraint in Lemma 2 is employed to achieve disturbance dissipativity by appropriately selecting the parameters for the general form in [25].

Lemma 2. The T-SFDEM (7) is called strictly input passive if the following relationship is satisfied with a positive scalar μ provided.

$$2 \sum_{k=0}^{k_T} e_y^T(k) w(k) > \mu \sum_{k=0}^{k_T} w^T(k) w(k) \quad (9)$$

where k_T denotes the terminal time.

Therefore, the energy consumption of the T-SFDEM (7) is greater than the disturbance energy by ensuring the relationship (9). However, the control effort is expected to increase significantly when the inequality conditions in (8) and (9) must be satisfied simultaneously. Considering practical control scenarios, the trade-off between state and input responses should also be carefully evaluated. Therefore, the optimal H_2 performance index is stated in Definition 2.

Definition 2. If the following condition is satisfied for the energy of state errors and control inputs, the H_2 performance index is optimized.

$$\min_k \left\{ \sum_{k=0}^{k_T} e_x^T(k) \mathbf{\Omega}_e e_x(k) + u^T(k) \mathbf{\Omega}_u u(k) \right\} \quad (10)$$

where $\mathbf{\Omega}_e$ and $\mathbf{\Omega}_u$ are the index matrices whose dimensions correspond to the states and inputs.

Thus, the control effort for the tracking purpose of the T-SFDEM (7) can be ensured not to become excessively large when multiple performance requirements are met. Therefore, the main tracking problem of nonlinear descriptor systems is to ensure the asymptotic stability of the tracking error $e_x(k)$ by applying the PDC-based P-D fuzzy tracking controller (6). Based on the closed-loop T-SFDEM (7), stability criteria can be proposed for the purpose $\lim_{k \rightarrow \infty} e_x(k) = 0$ so that the system state $x(k)$ of nonlinear descriptor systems can approach the desired state $x_d(k)$. Moreover, the disturbance dissipativity is guaranteed while achieving a better balance between tracking performance and control effort by satisfying the passivity constraint (9) and minimizing the H_2 performance (10) in the criteria.

The following section presents the P-D fuzzy tracking synthesis and stability analysis process for nonlinear descriptor systems.

3 Stability Criteria and Proportional-Difference Fuzzy Tracking Synthesis

By incorporating the robust control stated in Lemma 1, the passive constraint stated in Lemma 2, and the minimized H_2 performance stated in Definition 2, the stability criteria are proposed based on Lyapunov

theory and the closed-loop T-SFDEM (7). First, the sufficient conditions are derived in the following theorem to ensure the tracking objective and multiple performances.

Theorem 1. *The T-SFDEM (7) achieves the asymptotical stability, passive constraint (9) and minimization of H_2 performance (10) if there exist the positive definite matrices \mathbf{P} , $\mathbf{\Omega}_e$, $\mathbf{\Omega}_u$, the free-weighting matrices $\mathbf{\Xi}_p$, $\mathbf{\Xi}_d$ and the minimized scalar ρ such that the following sufficient conditions are satisfied with the given positive scalar μ .*

$$\begin{bmatrix} \Psi_{11} & \Psi_{12} & \mathbf{\Xi}_p \mathbf{W}_\alpha - \mathbf{C}_\alpha^T \\ * & \Psi_{22} & \mathbf{\Xi}_d \mathbf{W}_\alpha \\ * & * & \mu - \mathbf{V}_\alpha - \mathbf{V}_\alpha^T \end{bmatrix} < 0 \text{ for } \beta = \alpha = 1, 2, \dots, \tau \tag{11}$$

$$\begin{bmatrix} \tilde{\Psi}_{11} & \tilde{\Psi}_{12} & \mathbf{\Xi}_p \left(\frac{\mathbf{W}_\alpha + \mathbf{W}_\beta}{2} \right) - \left(\frac{\mathbf{C}_\alpha + \mathbf{C}_\beta}{2} \right)^T \\ * & \tilde{\Psi}_{22} & \mathbf{\Xi}_d \left(\frac{\mathbf{W}_\alpha + \mathbf{W}_\beta}{2} \right) \\ * & * & \mu - \left(\frac{\mathbf{V}_\alpha + \mathbf{V}_\beta}{2} \right) - \left(\frac{\mathbf{V}_\alpha + \mathbf{V}_\beta}{2} \right)^T \end{bmatrix} < 0 \text{ for } \beta > \alpha \tag{12}$$

$$\begin{bmatrix} -\rho & e_x^T(0) \\ * & -\mathbf{P}^{-1} \end{bmatrix} < 0 \tag{13}$$

where * denotes the transpose item in the matrix inequalities, $\text{sym}\{\Lambda\}$ denotes the sum of a matrix and its transpose $\Lambda + \Lambda^T$, and the symbols in the conditions (11) and (12) are stated below.

$$\begin{aligned} \Psi_{11} &= -\mathbf{P} + \text{sym} \left\{ \mathbf{\Xi}_p \hat{\mathbf{Q}}_{\alpha\alpha}^p \right\} + \mathbf{\Omega}_e + \mathbf{T}_\alpha^{pT} \mathbf{\Omega}_u \mathbf{T}_\alpha^p, \Psi_{12} = -\mathbf{\Xi}_p \hat{\mathbf{Q}}_{\alpha\alpha}^d + \hat{\mathbf{Q}}_{\alpha\alpha}^{pT} \mathbf{\Xi}_d^T - \mathbf{T}_\alpha^{pT} \mathbf{\Omega}_u \mathbf{T}_\alpha^d, \\ \Psi_{22} &= \mathbf{P} - \text{sym} \left\{ \mathbf{\Xi}_d \hat{\mathbf{Q}}_{\alpha\alpha}^d \right\} + \mathbf{T}_\alpha^{dT} \mathbf{\Omega}_u \mathbf{T}_\alpha^d, \tilde{\Psi}_{11} = -\mathbf{P} + \text{sym} \left\{ \mathbf{\Xi}_p \left(\frac{\hat{\mathbf{Q}}_{\alpha\beta}^p + \hat{\mathbf{Q}}_{\beta\alpha}^p}{2} \right) \right\} + \mathbf{\Omega}_e + \frac{\mathbf{T}_\alpha^{pT} \mathbf{\Omega}_u \mathbf{T}_\alpha^p + \mathbf{T}_\beta^{pT} \mathbf{\Omega}_u \mathbf{T}_\beta^p}{2}, \\ \tilde{\Psi}_{12} &= -\mathbf{\Xi}_p \left(\frac{\hat{\mathbf{Q}}_{\alpha\beta}^d + \hat{\mathbf{Q}}_{\beta\alpha}^d}{2} \right) + \left(\frac{\hat{\mathbf{Q}}_{\alpha\beta}^p + \hat{\mathbf{Q}}_{\beta\alpha}^p}{2} \right)^T \mathbf{\Xi}_d^T - \frac{\mathbf{T}_\alpha^{pT} \mathbf{\Omega}_u \mathbf{T}_\alpha^d + \mathbf{T}_\beta^{pT} \mathbf{\Omega}_u \mathbf{T}_\beta^d}{2}, \\ \text{and } \tilde{\Psi}_{22} &= \mathbf{P} - \text{sym} \left\{ \mathbf{\Xi}_d \left(\frac{\hat{\mathbf{Q}}_{\alpha\beta}^d + \hat{\mathbf{Q}}_{\beta\alpha}^d}{2} \right) \right\} + \frac{\mathbf{T}_\alpha^{dT} \mathbf{\Omega}_u \mathbf{T}_\alpha^d + \mathbf{T}_\beta^{dT} \mathbf{\Omega}_u \mathbf{T}_\beta^d}{2}. \end{aligned}$$

Proof of Theorem 1. To implement the stability analysis, the Lyapunov function is selected as

$$V(k) = e_x^T(k) \mathbf{P} e_x(k) \tag{14}$$

Thus, the first forward difference of the Lyapunov function (14) is derived with the following process.

$$\Delta V(k) = e_x^T(k+1) \mathbf{P} e_x(k+1) - e_x^T(k) \mathbf{P} e_x(k) \tag{15}$$

It is well known that the Lyapunov function (14) is defined in terms of the energy of the tracking error. As a result, the energy change is expressed by the derivative in (15). The stability analysis aims to achieve the tracking purpose by ensuring a negative energy change for (15). In addition, the technique of free-weighting matrix is also considered in the analysis process of this research to reduce the conservativeness. The equation for the free-weighting matrix is defined according to closed-loop T-SFDEM (7) as follows:

$$0 = 2 \left(e_x^T(k) \mathbf{\Xi}_p + e_x^T(k+1) \mathbf{\Xi}_d \right) \left(\sum_{\alpha=1}^{\tau} \sum_{\beta=1}^{\tau} \Phi_\alpha \Phi_\beta \left\{ -\hat{\mathbf{Q}}_{\alpha\beta}^d e_x(k+1) + \hat{\mathbf{Q}}_{\alpha\beta}^d e(k) + \mathbf{W}_\alpha w(k) \right\} \right) \tag{16}$$

Then, the following results are obtained by integrating (15) with the free-weighting Eq. (16).

$$\sum_{\alpha=1}^{\tau} \sum_{\beta=1}^{\tau} \Phi_{\alpha} \Phi_{\beta} \left\{ \mathbf{e}_x^T(k) \begin{bmatrix} -\mathbf{P} + \text{sym} \left\{ \Xi_p \hat{\mathbf{Q}}_{\alpha\beta}^p \right\} & -\Xi_p \hat{\mathbf{Q}}_{\alpha\beta}^d + \hat{\mathbf{Q}}_{\alpha\beta}^{pT} \Xi_d^T & \Xi_p \mathbf{W}_{\alpha} \\ * & \mathbf{P} - \text{sym} \left\{ \Xi_d \hat{\mathbf{Q}}_{\alpha\beta}^d \right\} & \Xi_d \mathbf{W}_{\alpha} \\ * & * & 0 \end{bmatrix} \mathbf{e}_x(k) \right\} \quad (17)$$

where $\mathbf{e}_x(k) = [e_x(k) \quad e_x(k+1) \quad w(k)]^T$.

With respect to the strictly input passive constraint (9), the cost function for the passivity analysis is defined as follows:

$$\mathbb{C}(k) = \sum_{k=0}^{k_T} (\mu w^T(k) w(k) - 2e_y^T(k) w(k)) \quad (18)$$

Considering $\Delta V(k)$ derived in the form of (17), the following relationship is obtained from the cost function (18) and the H_2 performance constraint under the zero-initial condition.

$$\begin{aligned} \mathbb{C}(k) &= \sum_{k=1}^{k_T} (\mu w^T(k) w(k) - 2e_y^T(k) w(k) + \Delta V(k)) - V(k_T) \\ &\leq \sum_{k=0}^{k_T} (\mu w^T(k) w(k) - 2e_y^T(k) w(k) + \Delta V(k)) \\ &\leq \sum_{k=0}^{k_T} (w^T(k) w(k) - 2e_y^T(k) w(k) + \Delta V(k) + e_x^T(k) \Omega_e e_x(k) + u^T(k) \Omega_u u(k)) \end{aligned} \quad (19)$$

Based on the P-D fuzzy tracking controller (6), the following result is obtained from the right-hand side of inequality (19).

$$\sum_{\alpha=1}^{\tau} \sum_{\beta=1}^{\tau} \Phi_{\alpha} \Phi_{\beta} \left\{ \mathbf{e}_x^T(k) \begin{bmatrix} -\mathbf{P} + \text{sym} \left\{ \Xi_p \hat{\mathbf{Q}}_{\alpha\beta}^p \right\} + \Omega_e & -\Xi_p \hat{\mathbf{Q}}_{\alpha\beta}^d + \hat{\mathbf{Q}}_{\alpha\beta}^{pT} \Xi_d^T - \mathbf{T}_{\beta}^{pT} \Omega_u \mathbf{T}_{\beta}^d & \Xi_p \mathbf{W}_{\alpha} - \mathbf{C}_{\alpha}^T \\ + \mathbf{T}_{\beta}^{pT} \Omega_u \mathbf{T}_{\beta}^p & * & * \\ * & \mathbf{P} - \text{sym} \left\{ \Xi_d \hat{\mathbf{Q}}_{\alpha\beta}^d \right\} + \mathbf{T}_{\beta}^{dT} \Omega_u \mathbf{T}_{\beta}^d & \Xi_d \mathbf{W}_{\alpha} \\ * & * & \mu - \mathbf{V}_{\alpha} - \mathbf{V}_{\alpha}^T \end{bmatrix} \mathbf{e}_x(k) \right\} \quad (20)$$

It is obvious that (20) becomes negative definite if the conditions (11) and (12) are satisfied by Theorem 1 according to the PDC concept. Then, the following results are also derived for the stability, passivity and H_2 performance.

From the relationship in (19), the cost function can be made negative ($\mathbb{C}(k) < 0$) when (20) is ensured to be negative definite. Compared with the strictly passive constraint in Lemma 2, the inequality (9) is satisfied accordingly. This also means that the T-SFDEM (7) has the ability to dissipate external disturbance energy. Then, the asymptotic stability can be proved by considering $w(k) = 0$. Therefore, Eq. (20) is reduced to the following form based on the setting.

$$\sum_{\alpha=1}^{\tau} \sum_{\beta=1}^{\tau} \Phi_{\alpha} \Phi_{\beta} \left\{ \begin{array}{c} \left[\begin{array}{c} e_x(k) \\ e_x(k+1) \end{array} \right]^T \left[\begin{array}{c} -\mathbf{P} + \text{sym} \left\{ \Xi_p \hat{\mathbf{Q}}_{\alpha\beta}^p \right\} \\ + \mathbf{\Omega}_e + \mathbf{T}_{\beta}^{pT} \mathbf{\Omega}_u \mathbf{T}_{\beta}^p \\ * \\ \mathbf{P} - \text{sym} \left\{ \Xi_d \hat{\mathbf{Q}}_{\alpha\beta}^d \right\} \\ + \mathbf{T}_{\beta}^{dT} \mathbf{\Omega}_u \mathbf{T}_{\beta}^d \end{array} \right] \left[\begin{array}{c} e_x(k) \\ e_x(k+1) \end{array} \right] \end{array} \right\} \quad (21)$$

It is observed that the negative definite of (21) also can be guaranteed by the conditions (11) and (12) in Theorem 1. Based on the properties of the free-weighting Eq. (16), $w(k) = 0$, and the property $e_x^T(k) \mathbf{\Omega}_e e_x(k) + u^T(k) \mathbf{\Omega}_u u(k) > 0$ of H_2 performance, the result of $\Delta V(k) < 0$ is thus achieved for (15). According to the Lyapunov theory, the asymptotic stability of the closed-loop T-SFDEM (7) is proved such that the convergence of tracking error energy can be achieved.

Consequently, the minimization of H_2 performance can be verified as follows. If the stability is ensured by Theorem 1, the following relationship can be derived from (15), (16) and (21).

$$\Delta V(k) + e_x^T(k) \mathbf{\Omega}_e e_x(k) + u^T(k) \mathbf{\Omega}_u u(k) < 0 \quad (22)$$

The following result is undoubtedly achieved with (22).

$$e_x^T(k) \mathbf{\Omega}_e e_x(k) + u^T(k) \mathbf{\Omega}_u u(k) < -\Delta V(k) \quad (23)$$

The following relationship is derived by employing the cumulative sum on both sides of inequality (23) due to the convergence of the state error dynamic.

$$\sum_{k=0}^{k_T} \left(e_x^T(k) \mathbf{\Omega}_e e_x(k) + u^T(k) \mathbf{\Omega}_u u(k) \right) < e_x^T(0) \mathbf{P} e_x(0) \quad (24)$$

Then, the following relationship can be obtained from inequality (24) if the condition (13) is satisfied by Theorem 1.

$$\sum_{k=0}^{k_T} \left(e_x^T(k) \mathbf{\Omega}_e e_x(k) + u^T(k) \mathbf{\Omega}_u u(k) \right) < e_x^T(0) \mathbf{P} e_x(0) < \min(\rho) \quad (25)$$

From the relationship in (25), it can be observed that the H_2 performance index is minimized under condition (13) by Theorem 1. This indicates that the trade-off between state and input responses can be optimized while ensuring stability and disturbance dissipativity. □

However, the sufficient conditions in Theorem 1 remain in a non-LMI form and involve time-varying uncertainties. To transform Theorem 1 into an LMI problem solvable by computational programs, the Schur complement and Lemma 1 are applied in the following theorem.

Theorem 2. *The T-SFDEM (7) achieves the asymptotical stability, passive constraint (9), robustness and minimization of H_2 performance (10) if there exist the positive definite matrices \mathbf{Z} , \mathbf{U}_e , \mathbf{U}_u , the matrices σ_1 , σ_2 , \mathbf{Y}_{β} , \mathbf{G}_{β} , the positive scalar ω and the minimized scalar ρ such that the following sufficient conditions are satisfied with the given positive scalar μ .*

$$\begin{bmatrix} -\mathbf{Z} & \Theta_{12} & -\mathbf{Z}\mathbf{C}_\alpha^T & \mathbf{Y}_\alpha^T & \sigma_1^T & \mathbf{Z} & \Theta_{17} \\ * & \Theta_{22} & -\mathbf{W}_\alpha & -\mathbf{G}_\alpha^T & \sigma_2^T & 0 & \Theta_{27} \\ * & * & \mu - \mathbf{V}_\alpha - \mathbf{V}_\alpha^T & 0 & 0 & 0 & 0 \\ * & * & * & -\Omega_u^{-1} & 0 & 0 & 0 \\ * & * & * & * & -\mathbf{Z} & 0 & 0 \\ * & * & * & * & * & -\Omega_e^{-1} & 0 \\ * & * & * & * & * & * & -\omega \end{bmatrix} < 0 \text{ for } \beta = \alpha = 1, 2, \dots, \tau \tag{26}$$

$$\begin{bmatrix} -\mathbf{Z} & \tilde{\Theta}_{12} & -\mathbf{Z} \left(\frac{\mathbf{C}_\alpha + \mathbf{C}_\beta}{2} \right)^T & \left(\frac{\mathbf{Y}_\alpha + \mathbf{Y}_\beta}{2} \right)^T & \sigma_1^T & \mathbf{Z} & \tilde{\Theta}_{17} \\ * & \tilde{\Theta}_{22} & - \left(\frac{\mathbf{W}_\alpha + \mathbf{W}_\beta}{2} \right) & - \left(\frac{\mathbf{G}_\alpha + \mathbf{G}_\beta}{2} \right)^T & \sigma_2^T & 0 & \tilde{\Theta}_{27} \\ * & * & \mu - \left(\frac{\mathbf{V}_\alpha + \mathbf{V}_\beta}{2} \right) - \left(\frac{\mathbf{V}_\alpha + \mathbf{V}_\beta}{2} \right)^T & 0 & 0 & 0 & 0 \\ * & * & * & -\mathbf{U}_u & 0 & 0 & 0 \\ * & * & * & * & -\mathbf{Z} & 0 & 0 \\ * & * & * & * & * & -\mathbf{U}_e & 0 \\ * & * & * & * & * & * & -\omega \end{bmatrix} < 0 \text{ for } \beta > \alpha \tag{27}$$

$$\begin{bmatrix} -\rho & e_x^T(0) \\ * & -\mathbf{Z} \end{bmatrix} < 0 \tag{28}$$

where $\mathbf{U}_e = \Omega_e^{-1}$, $\mathbf{U}_u = \Omega_u^{-1}$, and the symbols in the conditions (26) and (27) are stated below.

$$\begin{aligned} \Theta_{12} &= -\mathbf{Z}\mathbf{A}_\alpha^T - \mathbf{Y}_\alpha^T\mathbf{B}_\alpha^T + \sigma_1^T\mathbf{E}_\alpha^T, & \Theta_{22} &= \text{sym} \left\{ \sigma_2^T\mathbf{E}_\alpha^T + \mathbf{G}_\alpha^T\mathbf{B}_\alpha^T \right\} + \omega\mathbf{H}_\alpha\mathbf{H}_\alpha^T, & \Theta_{17} &= -\mathbf{Z}\mathbf{R}_{A\alpha}^T - \mathbf{Y}_\alpha^T\mathbf{R}_{B\alpha}^T + \sigma_1^T\mathbf{R}_{\Sigma\alpha}^T, \\ \Theta_{27} &= \sigma_2^T\mathbf{R}_{\Sigma\alpha}^T + \mathbf{G}_\alpha^T\mathbf{R}_{B\alpha}^T, & \tilde{\Theta}_{12} &= -\mathbf{Z} \left(\frac{\mathbf{A}_\alpha + \mathbf{A}_\beta}{2} \right)^T - \left(\frac{\mathbf{Y}_\beta^T\mathbf{B}_\alpha^T + \mathbf{Y}_\alpha^T\mathbf{B}_\beta^T}{2} \right) + \sigma_1^T \left(\frac{\mathbf{E}_\alpha + \mathbf{E}_\beta}{2} \right)^T, \\ \tilde{\Theta}_{22} &= \text{sym} \left\{ \sigma_2^T \left(\frac{\mathbf{E}_\alpha + \mathbf{E}_\beta}{2} \right)^T + \left(\frac{\mathbf{G}_\beta^T\mathbf{B}_\alpha^T + \mathbf{G}_\alpha^T\mathbf{B}_\beta^T}{2} \right) \right\} + \omega \left(\frac{\mathbf{H}_\alpha\mathbf{H}_\alpha^T + \mathbf{H}_\beta\mathbf{H}_\beta^T}{2} \right), \\ \tilde{\Theta}_{17} &= -\mathbf{Z} \left(\frac{\mathbf{R}_{A\alpha} + \mathbf{R}_{A\beta}}{2} \right)^T - \left(\frac{\mathbf{Y}_\beta^T\mathbf{R}_{B\alpha}^T + \mathbf{Y}_\alpha^T\mathbf{R}_{B\beta}^T}{2} \right) + \sigma_1^T \left(\frac{\mathbf{R}_{\Sigma\alpha} + \mathbf{R}_{\Sigma\beta}}{2} \right)^T, \\ \tilde{\Theta}_{27} &= \sigma_2^T \left(\frac{\mathbf{R}_{\Sigma\alpha} + \mathbf{R}_{\Sigma\beta}}{2} \right)^T + \left(\frac{\mathbf{G}_\beta^T\mathbf{R}_{B\alpha}^T + \mathbf{G}_\alpha^T\mathbf{R}_{B\beta}^T}{2} \right), & \mathbf{Y}_\alpha &= \mathbf{T}_\alpha^p\mathbf{Z} - \mathbf{T}_\alpha^d\sigma_1, & \mathbf{Y}_\beta &= \mathbf{T}_\beta^p\mathbf{Z} - \mathbf{T}_\beta^d\sigma_1, & \mathbf{G}_\alpha &= \mathbf{T}_\alpha^d\sigma_2, & \mathbf{G}_\beta &= \mathbf{T}_\beta^d\sigma_2, & \sigma_1 &= \\ & & & & & & & & & & & -\mathbf{E}_d^{-T}\mathbf{E}_p^T\mathbf{Z}, & \sigma_2 &= -\mathbf{E}_d^{-T} \text{ and } \mathbf{Z} = \mathbf{P}^{-1}. \end{aligned}$$

Proof of Theorem 2. In the proof of Theorem 2, the derivation process for the condition (26) is only presented as an example. In other words, the condition (27) can be derived through a similar process. According to the Schur complement lemma, the following inequality is obtained from (26) if the condition (26) is satisfied by the stability criteria in Theorem 2.

$$\begin{bmatrix} -\mathbf{Z} & \Theta_{12} & -\mathbf{Z}\mathbf{C}_\alpha^T & \mathbf{Y}_\alpha^T & \sigma_1^T & \mathbf{Z} \\ * & \text{sym} \left\{ \sigma_2^T\mathbf{E}_\alpha^T + \mathbf{G}_\alpha^T\mathbf{B}_\alpha^T \right\} & -\mathbf{W}_\alpha & -\mathbf{G}_\alpha^T & \sigma_2^T & 0 \\ * & * & \mu - \mathbf{V}_\alpha - \mathbf{V}_\alpha^T & 0 & 0 & 0 \\ * & * & * & -\Omega_u^{-1} & 0 & 0 \\ * & * & * & * & -\mathbf{Z} & 0 \\ * & * & * & * & * & -\Omega_e^{-1} \end{bmatrix}$$

$$+ \omega \begin{bmatrix} 0 \\ \mathbf{H}_\alpha \\ 0 \\ 0 \\ 0 \\ 0 \end{bmatrix} \begin{bmatrix} 0 & \mathbf{H}_\alpha^T & 0 & 0 & 0 & 0 \end{bmatrix} + \omega^{-1} \begin{bmatrix} \Theta_{17} \\ \Theta_{27} \\ 0 \\ 0 \\ 0 \\ 0 \end{bmatrix} \begin{bmatrix} \Theta_{17}^T & \Theta_{27}^T & 0 & 0 & 0 & 0 \end{bmatrix} < 0 \tag{29}$$

Then, the following condition is also satisfied by condition (26) due to (29) and inequality (8) in Lemma 1.

$$\begin{bmatrix} -\mathbf{Z} & -\mathbf{Z}\hat{\mathbf{Q}}_{\alpha\beta}^{p^T} + \sigma_1^T \hat{\mathbf{Q}}_{\alpha\beta}^{d^T} & -\mathbf{Z}\mathbf{C}_\alpha^T & \mathbf{Y}_\alpha^T & \sigma_1^T & \mathbf{Z} \\ * & \text{sym} \left\{ \sigma_2^T \hat{\mathbf{Q}}_{\alpha\beta}^{d^T} \right\} & -\mathbf{W}_\alpha & -\mathbf{G}_\alpha^T & \sigma_2^T & 0 \\ * & * & \mu - \mathbf{V}_\alpha - \mathbf{V}_\alpha^T & 0 & 0 & 0 \\ * & * & * & -\mathbf{\Omega}_u^{-1} & 0 & 0 \\ * & * & * & * & -\mathbf{Z} & 0 \\ * & * & * & * & * & -\mathbf{\Omega}_e^{-1} \end{bmatrix} < 0 \tag{30}$$

It is evident that the time-varying terms in the uncertainties of (30) can be successfully transformed into a constant form in (29) for LMI analysis through Lemma 1. With the application Schur complement, the condition (30) is further transferred into the following form.

$$\begin{bmatrix} -\mathbf{Z} + \mathbf{Z}\mathbf{\Omega}_e\mathbf{Z} + \sigma_1^T \mathbf{Z}^{-1} \sigma_1 + \mathbf{Y}_\alpha^T \mathbf{\Omega}_u \mathbf{Y}_\alpha & -\mathbf{Z}\hat{\mathbf{Q}}_{\alpha\beta}^{p^T} + \sigma_1^T \hat{\mathbf{Q}}_{\alpha\beta}^{d^T} + \sigma_1^T \mathbf{Z}^{-1} \sigma_2 - \mathbf{Y}_\alpha^T \mathbf{\Omega}_u \mathbf{G}_\alpha & -\mathbf{Z}\mathbf{C}_\alpha^T \\ * & \text{sym} \left\{ \sigma_2^T \hat{\mathbf{Q}}_{\alpha\beta}^{d^T} \right\} + \sigma_2^T \mathbf{Z}^{-1} \sigma_2 + \mathbf{G}_\alpha^T \mathbf{\Omega}_u \mathbf{G}_\alpha & -\mathbf{W}_\alpha \\ * & * & \mu - \mathbf{V}_\alpha - \mathbf{V}_\alpha^T \end{bmatrix} < 0 \tag{31}$$

According to the definitions of \mathbf{Y}_α , \mathbf{G}_α , σ_1 , σ_2 , and \mathbf{Z} , the left-hand side of inequality (31) is obtained from condition (11) by pre- and post-multiplying the following matrices:

$$\begin{bmatrix} \mathbf{P}^{-1} & -\mathbf{P}^{-1} \mathbf{\Xi}_p \mathbf{\Xi}_d^{-1} & 0 \\ 0 & -\mathbf{\Xi}_d^{-1} & 0 \\ 0 & 0 & \mathbf{I} \end{bmatrix} \text{ and } \begin{bmatrix} \mathbf{P}^{-1} & -\mathbf{P}^{-1} \mathbf{\Xi}_p \mathbf{\Xi}_d^{-1} & 0 \\ -\mathbf{\Xi}_d^{-T} \mathbf{\Xi}_p^T \mathbf{P}^{-1} & -\mathbf{\Xi}_d^{-T} & 0 \\ 0 & 0 & \mathbf{I} \end{bmatrix} \tag{32}$$

As a result, it is derived that the condition (11) in Theorem 1 can be satisfied if the inequality (31) holds, which can be guaranteed by the condition (26) in Theorem 2 following the analysis process from (29) to (32). Analogously, the condition (12) in Theorem 1 can be ensured by the condition (27) in Theorem 2. In compliance with the analysis process of Theorem 1 and Lyapunov theory, the asymptotic stability of the tracking error subject to multiple constraints is achieved by satisfying conditions (11)–(13), which are ensured by the LMI conditions (26)–(28). □

Therefore, it is concluded that the closed-loop T-SFDEM (7) achieves the asymptotic stability, passivity, robustness and minimized H_2 performance simultaneously if the conditions (26)–(28) are all satisfied by the P-D fuzzy tracking synthesis of Theorem 2. Moreover, the conditions (26)–(28) presented in LMI form are solved and the feasible solutions are conveniently derived using the convex optimization algorithm in MATLAB or other software. As a final point, the computational complexity of the proposed design process is discussed in the following remark.

Remark 2. *The computational complexity of the T-SFDM-based fuzzy control and P-D feedback technique in tracking synthesis for nonlinear descriptor systems can be summarized in the following points:*

- [I] *The application of the T-SFDM (1), (2) and T-SFDEM (5) within the T-SFM framework can represent nonlinear descriptor systems as several linear subsystems. Therefore, the control problem of nonlinear descriptor systems can be tackled using linear techniques. This feature reduces the complexity and computational requirements in designing a tracking synthesis.*
- [II] *Corresponding to the T-SFM, the fuzzy controller is also constructed within a linear framework based on the PDC concept. It is noted that the PDC-based fuzzy controller are blended to obtain the overall fuzzy controller (6), which are linear combinations of membership functions and linear sub-controllers. This advantage enables the fuzzy tracking controller to be applied in a linear framework and reduces the computational complexity when controlling nonlinear descriptor systems.*
- [III] *Based on the T-SFDEM (5) and the fuzzy controller (6), the fuzzy tracking synthesis can be conveniently converted into an LMI problem, as presented in Theorem 2. It is well known that the LMI problem can be easily solved by the computational program so that the computational complexity of tracking synthesis for nonlinear descriptor systems can be reduced.*
- [IV] *The P-D feedback technique, which plays an important role in the fuzzy tracking controller (6), can efficiently transfer the control problem of systems in descriptor form into a general problem. This advantage reduces the design complexity of tracking synthesis for nonlinear descriptor systems, as presented in Theorems 1 and 2.*

Although the tracking synthesis under the T-SFM and PDC framework can efficiently reduce the computational complexity, some questions still remain to be discussed. From [43], it is known that the computational complexity may gradually increase while ensuring the approximation accuracy. This is due to the increased number of variables in the antecedent part and fuzzy rules. However, the number of these factors is often not large for practical nonlinear systems, which is observed in the later section.

Before the simulation begins, the following algorithm is provided to make the application of the proposed fuzzy tracking synthesis clearer.

From Lemma 2, it can be known that a larger parameter μ leads to a more conservative analysis process, although better disturbance dissipativity can be achieved. Moreover, the preservation of control effort is somewhat contrary to the ability to handle disturbance effects. This characterization makes the control problem in Theorem 2 more difficult to solve. Therefore, the value of the parameter is required to be decreased if feasible solutions cannot be obtained by the solver in Step 3. Based on the design process introduced in Algorithm 1, two simulation examples are provided to demonstrate the feasibility and applicability of Theorem 2.

Algorithm 1: P-D fuzzy controller design process

Step 1: Check whether the system meets the definitions and assumptions.

Step 2: Selecting the parameter μ for the passive constraint (9), the variables \mathbf{Z} , \mathbf{U}_e , \mathbf{U}_u , $\boldsymbol{\sigma}_1$, $\boldsymbol{\sigma}_2$, \mathbf{Y}_β , \mathbf{G}_β are obtained by solving Theorem 2 and minimizing ρ with the minimization solver in LMI toolbox of MATLAB.

Step 3: Check whether the result is feasible. If not, decrease the value of the parameter μ and return to Step 2. If it is, the feasible solutions are obtained, and proceed to Step 4.

Step 4: With the definition of $\mathbf{Y}_\beta = \mathbf{T}_\beta^p \mathbf{Z} - \mathbf{T}_\beta^d \boldsymbol{\sigma}_1$ and $\mathbf{G}_\beta = \mathbf{T}_\beta^d \boldsymbol{\sigma}_2$ in Theorem 2, the control gains \mathbf{T}_β^d and \mathbf{T}_β^p can be calculated by using the feasible solutions of variables \mathbf{Z} , $\boldsymbol{\sigma}_1$, $\boldsymbol{\sigma}_2$, \mathbf{Y}_β , \mathbf{G}_β .

Step 5: Applying the P-D fuzzy controller (6) with the calculated gains \mathbf{T}_β^d and \mathbf{T}_β^p to the nonlinear descriptor system, simulation results can be obtained.

4 Simulations and Discussions

The tracking control problem for nonlinear descriptor systems is addressed by a fuzzy tracking synthesis proposed in Theorem 2, which satisfies multiple requirements, including asymptotic stability, passivity, robustness, and the optimization between state responses and control efforts. Based on the representation of the T-SFDEM (7), two simulation examples are provided. The first example involves a singular-type system based on the equivalent circuit model of a DC motor. Moreover, the comparison results with the existing research are also provided to demonstrate the effectiveness of combining multiple performance constraints. To verify the effectiveness of the controller design approach based on descriptor form, the second example examines a general-type system derived from the discretized ship steering model. First, the simulation results of the DC motor compared with [44] are provided as follows.

Example 1. Referring to [45,46], the singular nonlinear mathematical model is given as follows for the equivalent circuit system of the DC motor, with the consideration of uncertainties and disturbances.

$$(3 + \Delta_{e1}(k)) x_1(k+1) = 2.85x_1(k) + x_3(k) - 2u_1(k) - 0.8w(k) \tag{33}$$

$$(3 + \Delta_{e2}(k)) x_2(k+1) = 0.0225x_1(k) x_2(k) + (1.875 + \Delta_{a22}(k)) x_2(k) + 3u_1(k) + 0.5w(k) \tag{34}$$

$$x_3(k) = (0.03 + \Delta_{a32}(k)) x_2^2(k) - 0.8w(k) - u_1(k) - (4 + \Delta_{b32}(k)) u_2(k) \tag{35}$$

where $x_1(k)$ is the angular velocity, $x_2(k)$ is the current of equivalent circuit, and the expression $x_3(k) = \left(\frac{Km \cdot Lf \cdot t}{J}\right) x_2^2(k) - u_1(k) - 4u_2(k)$ represents the algebraic constraint associated with the current energy characteristics of the DC motor in [45], Km , Lf , t , J respectively denote the torque/back emf constant, the field winding inductance, the sampling time and the moment of inertia, $u_1(k)$ is the load torque and $u_2(k)$ is the input voltage.

Remark 3. For the control issue of the nonlinear DC motor (33)–(35), the uncertain factors $\Delta_{a22}(k) = 0.01875\sin(k)$, $\Delta_{a32}(k) = 0.0003\sin(k)$, $\Delta_{b32}(k) = 0.04\sin(k)$ and $\Delta_{e1}(k) = \Delta_{e2}(k) = 0.3\sin(k)$ are considered to account for the effect of temperature on the circuit's current. Additionally, the disturbance $w(k)$ is introduced to represent external influences from the environment or human interaction.

Based on references [45,46] and related research [47], it is known that the mathematical model (33)–(35) has been established for a series DC motor. This type of motor has been efficiently applied in electric traction systems, such as electric buses and subways, which require large initial torque. However, these applications often face uncertainties such as wear and tear, as well as disturbances from rough roads. As a result, the control efficiency of series DC motors must be improved.

Considering the operating range $x_2(k) \in [-3.5, 3.5]$ for the nonlinearities, the T-SFDM of the nonlinear descriptor system (33)–(35) is constructed as follows:

$$\begin{cases} \sum_{\alpha=1}^2 \Phi_{\alpha} \left\{ \hat{\mathfrak{T}}_{\alpha} x(k+1) \right\} = \sum_{\alpha=1}^2 \Phi_{\alpha} \left\{ \hat{\mathbf{A}}_{\alpha} x(k) + \hat{\mathbf{B}}_{\alpha} u(k) + \mathbf{W}_{\alpha} w(k) \right\} \\ y(k) = \sum_{\alpha=1}^2 \Phi_{\alpha} \left\{ \mathbf{C}_{\alpha} x(k) + \mathbf{V}_{\alpha} w(k) \right\} \end{cases} \quad (36)$$

where $x(k) = [x_1(k) \ x_2(k) \ x_3(k)]^T$, $u(k) = [u_1(k) \ u_2(k)]^T$ and the model matrices are presented as follows:

$$\begin{aligned} \mathfrak{T}_1 = \mathfrak{T}_2 = \begin{bmatrix} 3 & 0 & 0 \\ 0 & 3 & 0 \\ 0 & 0 & 0 \end{bmatrix}, \mathbf{A}_1 = \begin{bmatrix} 2.85 & 0 & 3 \\ 0.0788 & 1.8750 & 0 \\ 0 & -0.1050 & -1 \end{bmatrix}, \mathbf{A}_2 = \begin{bmatrix} 2.85 & 0 & 3 \\ -0.0788 & 1.8750 & 0 \\ 0 & 0.1050 & -1 \end{bmatrix} \\ \mathbf{B}_1 = \mathbf{B}_2 = \begin{bmatrix} -2 & 0 \\ 3 & 0 \\ -1 & -4 \end{bmatrix}, \mathbf{C}_1 = \mathbf{C}_2 = [0 \ 0 \ 1], \mathbf{W}_1 = \mathbf{W}_2 = \begin{bmatrix} 0.8 \\ 0.5 \\ 0.8 \end{bmatrix} \text{ and } \mathbf{V}_1 = \mathbf{V}_2 = 0. \end{aligned} \quad (37)$$

The uncertain matrices are also constructed with the following components.

$$\begin{aligned} \mathbf{H}_1 = \mathbf{H}_2 = \begin{bmatrix} 0.1 & 0 & 0 \\ 0 & 0.1 & 0 \\ 0 & 0 & 0.1 \end{bmatrix}, \mathbf{R}_{\mathfrak{T}_1} = \mathbf{R}_{\mathfrak{T}_2} = \begin{bmatrix} 3 & 0 & 0 \\ 0 & 3 & 0 \\ 0 & 0 & 0 \end{bmatrix}, \mathbf{R}_{\mathbf{A}_1} = \begin{bmatrix} 0 & 0 & 0 \\ 0 & 0.1875 & 0 \\ 0 & -0.0105 & 0 \end{bmatrix}, \\ \mathbf{R}_{\mathbf{A}_2} = \begin{bmatrix} 0 & 0 & 0 \\ 0 & 0.1875 & 0 \\ 0 & 0.0105 & 0 \end{bmatrix}, \mathbf{R}_{\mathbf{B}_1} = \mathbf{R}_{\mathbf{B}_2} = \begin{bmatrix} 0 & 0 \\ 0 & 0 \\ 0 & -0.4 \end{bmatrix}, \text{ and } \Delta_1(k) = \Delta_2(k) = \sin(k). \end{aligned} \quad (38)$$

Obviously, the time-varying uncertain terms $\Delta_1(k)$ and $\Delta_2(k)$ satisfy the prerequisite specified in Lemma 1. Based on the operating range of $x_2(k)$, the membership function is given for the T-SFDM (36)–(38) in Fig. 1.

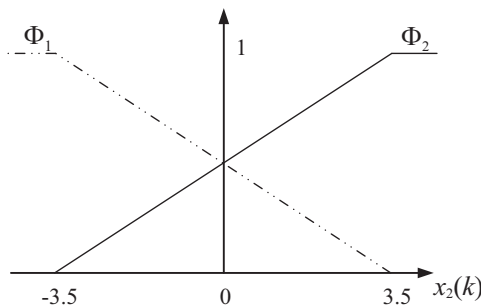


Figure 1: Membership function of nonlinear DC motor system

With the same membership function in Fig. 1 and the same matrices as (37) and (38), the target model can also be constructed in the form of (4), along with the target state trajectories for the nonlinear descriptor DC motor system (33)–(35). Based on the T-SFDM with uncertainties (36)–(38), the comparison results

between the proposed fuzzy tracking synthesis in Theorem 2 and [44] are provided in solving the typical convergence issue as follows.

In the simulation of Example 1, the typical convergence benchmark for the DC motor is considered to more clearly demonstrate the effectiveness of the designed P-D fuzzy controller under multiple performance criteria. In other words, $x_d(k)$ is set to the zero vector. Given the parameter $\mu = 0.1$ and the initial condition $x(0) = [20^\circ/s \ 0 \ 0]^T$, the following control gains are obtained by solving the LMI control problem in Theorem 2 using MATLAB and Algorithm 1.

$$\begin{aligned} \mathbf{T}_1^p &= \begin{bmatrix} 0.6213 & -0.0026 & -1.8922 \\ 1.0440 & 0.1741 & -18.2543 \end{bmatrix}, \mathbf{T}_2^p = \begin{bmatrix} 0.5841 & 0.0234 & -2.1361 \\ 0.9909 & 0.1955 & -17.2680 \end{bmatrix}, \\ \mathbf{T}_1^d &= \begin{bmatrix} -9.9094 & -1.099 & -165.4071 \\ -27.7294 & -13.8171 & -736.1034 \end{bmatrix}, \mathbf{T}_2^d = \begin{bmatrix} -9.5387 & -1.1170 & -161.4641 \\ -26.1619 & -13.017 & -693.7475 \end{bmatrix}. \end{aligned} \tag{39}$$

Moreover, the matrices in the minimized H_2 performance (10) is obtained as follows:

$$\mathbf{\Omega}_e = \begin{bmatrix} 0.0105 & 0.0003 & 0.0004 \\ 0.0003 & 0.0085 & 0.0002 \\ 0.0004 & 0.0002 & 0.0126 \end{bmatrix} \text{ and } \mathbf{\Omega}_u = \begin{bmatrix} 0.0109 & 0.0004 \\ 0.0004 & 0.0122 \end{bmatrix}. \tag{40}$$

In addition, the control gains and H_2 performance matrices are also obtained by [44]. Note that only the H_2 performance is considered in the P-D fuzzy controller design of [44] under uncertainties. Although the control performance can be ensured while preserving the control effort, the designed fuzzy controller is insufficient to overcome the disturbance effects due to this preservation. Solving the controller design problem in [44] with MATLAB, the gains are presented as follows:

$$\begin{aligned} \mathbf{F}_1^p &= \begin{bmatrix} 0.1636 & 0.0045 & 0.0462 \\ 0.7597 & 0.0049 & 0.2134 \end{bmatrix}, \mathbf{F}_2^p = \begin{bmatrix} 0.1371 & 0.0017 & 0.0381 \\ 0.5746 & 0.0020 & 0.1539 \end{bmatrix}, \\ \mathbf{F}_1^d &= \begin{bmatrix} 5.1556 & -0.0411 & 17.0249 \\ 24.3057 & -0.3913 & 79.6177 \end{bmatrix}, \mathbf{F}_2^d = \begin{bmatrix} 4.3365 & -0.0470 & 14.2765 \\ 18.4575 & -0.2939 & 60.4652 \end{bmatrix}. \end{aligned} \tag{41}$$

The matrices in the minimized H_2 performance is presented as follows:

$$\mathbf{\Omega}_e = 10^{-3} \times \begin{bmatrix} 0.2604 & 0.0004 & 0.0249 \\ 0.0004 & 0.2439 & -0.0005 \\ 0.0249 & -0.0005 & 0.3070 \end{bmatrix} \text{ and } \mathbf{\Omega}_u = \begin{bmatrix} 0.1478 & -0.0072 \\ -0.0072 & 0.1239 \end{bmatrix}. \tag{42}$$

It should be noted that the symbol \mathbf{F} for control gains in (41) is equivalent to the symbol \mathbf{T} in this research since the typical convergence problem is considered. Comparing the results (39), (40) and (41), (42), it is obvious that the control gains obtained by [44] are smaller than obtained by the proposed fuzzy control approach. This is because the additional passive constraint must be satisfied in Theorem 2 to achieve the dissipativity of the disturbance energy. Similarly, the matrices in (42) are smaller than in (40) since the H_2 performance index is difficult to be minimized when the passive constraint is considered simultaneously.

To better demonstrate the control performance of the proposed method compared to [44], the disturbance is shown in Fig. 2, which includes a square wave and an impulse signal. Therefore, the state responses are presented in Figs. 3–5 by applying the P-D fuzzy controller respectively with the gains (39) and (41) in the form of (6) to the nonlinear descriptor DC system (33)–(35).

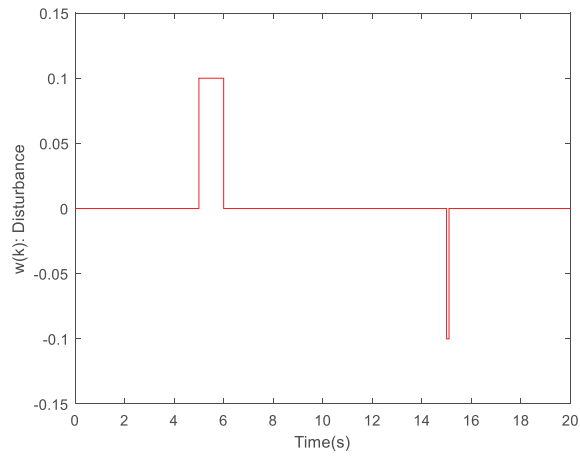


Figure 2: Disturbance of nonlinear DC motor system

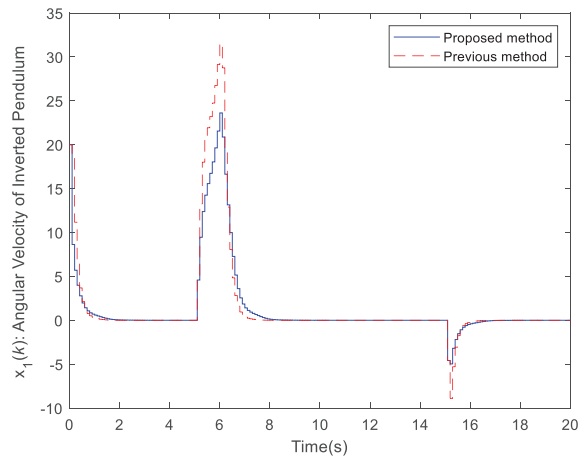


Figure 3: State $x_1(k)$ responses compared with [44]

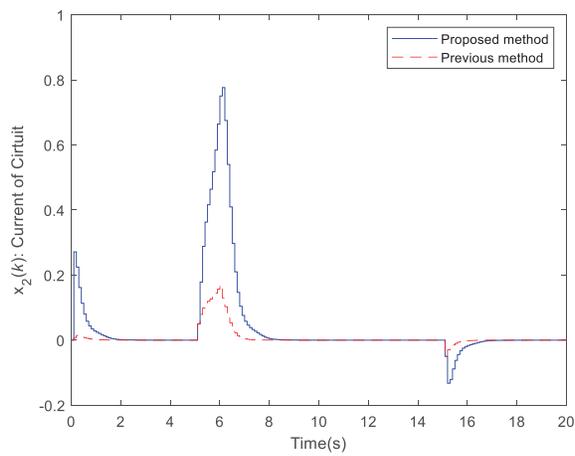


Figure 4: State $x_2(k)$ responses compared with [44]

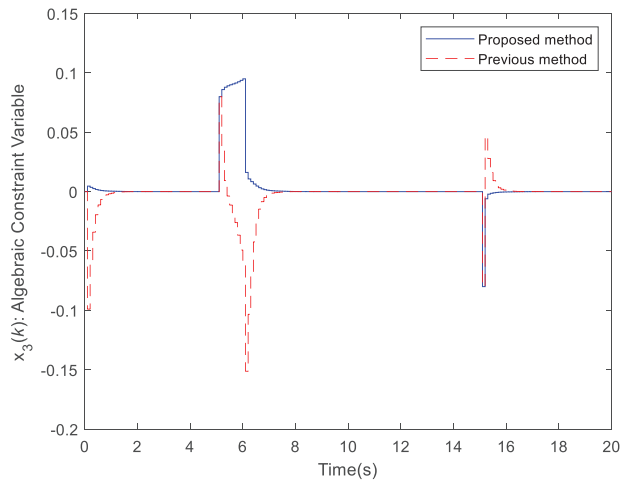


Figure 5: State $x_3(k)$ responses compared with [44]

From Figs. 3–5, it can be observed that the system states achieve asymptotic stability by using both fuzzy control methods even under the influence of uncertainties and disturbances. However, the responses affected by disturbances are more drastic when using the method from [44] in Figs. 3 and 5. This is because only the minimized H_2 performance is considered and results in smaller control effort that cannot effectively handle the disturbance effects. Note that these drastic changes may cause redundant wear and tear in the equipment. Although the larger overshoots are caused in Fig. 4 by the P-D fuzzy controller designed in this research, they are still relatively smaller than the overshoots in Fig. 3 when using [44]. Therefore, it can be said that the proposed multiple performance-constrained fuzzy control synthesis in Theorem 2 provides more reliable system responses for practical nonlinear descriptor systems under the effect of singularities, uncertainties, and disturbances.

To more clearly demonstrate the effectiveness of the proposed method, the comparison results of the evaluation indices are presented in Table 1. Before the table is given, the following symbols are defined for the different evaluation indices.

$$\begin{aligned}
 \Upsilon_{passive} &= \frac{\mu \sum_{k=0}^{k_T} w^T(k) w(k)}{2 \sum_{k=0}^{k_T} e_y^T(k) w(k)}, \quad \Upsilon_{H2} = \sum_{k=0}^{k_T} e_x^T(k) \Omega_e e_x(k) + u^T(k) \Omega_u u(k) \\
 \Upsilon_{MSE}^n &= \frac{1}{k_T} \sum_{k=0}^{k_T} (x_n(k) - x_{nd}(k))^2, \quad \Upsilon_{MAE}^n = \frac{1}{k_T} \sum_{k=0}^{k_T} |x_n(k) - x_{nd}(k)|
 \end{aligned} \tag{43}$$

where MSE denotes the mean squared error, MAE denotes the mean absolute error, k_T denotes the terminal time which is 20 in this simulation, $n = 1, 2, 3$ denote the state numbers. Note that $x_{nd}(k)$ are all set as zero in the typical convergence problem.

Based on the definition (43) and matrices in (42), Table 1 is presented as follows.

Table 1: Evaluation indices of comparison results

Methods	Passivity	H ₂ performance	MSE	MAE
Proposed method	$Y_{passive} = 0.07488$	$Y_{H2} = 53.4460$ $< \rho = 55.2689$	$\begin{cases} Y_{MSE}^1 = 22.0016 \\ Y_{MSE}^2 = 0.0208 \\ Y_{MSE}^3 = 4.3566 \times 10^{-4} \end{cases}$	$\begin{cases} Y_{MAE}^1 = 1.5678 \\ Y_{MAE}^2 = 0.0477 \\ Y_{MAE}^3 = 0.0053 \end{cases}$
Method in [44]	$Y_{passive} = 0.4199$	$Y_{H2} = 27.7940$ $< \rho = 39.9910$	$\begin{cases} Y_{MSE}^1 = 38.2502 \\ Y_{MSE}^2 = 9.7740 \times 10^{-4} \\ Y_{MSE}^3 = 4.8480 \times 10^{-4} \end{cases}$	$\begin{cases} Y_{MAE}^1 = 1.9255 \\ Y_{MAE}^2 = 0.0093 \\ Y_{MAE}^3 = 0.0059 \end{cases}$

From the results in Table 1, it is not difficult to find that the MSE and MAE values of the first and third states are smaller when applying the method, while those of the second state are larger. This trend is also observed in Figs. 3–5. Moreover, the value Y_{H2} calculated according to the definition of H₂ performance (10) by applying the proposed method is larger than that obtained by applying [44]. This is because the passive constraint must also be satisfied. According to the passive constraint (9) defined in Lemma 2, the value of $Y_{passive}$ must be less than 1. It is observed that both P-D fuzzy control methods achieve this goal. However, the value obtained by the proposed method is smaller, which indicates that the energy consumption relative to the disturbance input energy is higher compared to the method in [44]. Therefore, the P-D fuzzy controller designed by Theorem 2 can achieve the better trade-off between the state convergence rate and control effort when stabilizing the DC motor system (33)–(35) even under the uncertainty and disturbance effects.

In the next example, a nonlinear ship steering system modeled in a typical form is considered for the simulation to verify the P-D fuzzy tracking synthesis based on the descriptor system.

Example 2. In the second example, the following discretized nonlinear ship steering model is presented by extending the results from [44] with the additional consideration of uncertainties and disturbances.

$$x_1(k+1) = x_1(k) + 0.1\cos(x_3(k))x_4(k) - 0.1\sin(x_3(k))x_5(k) \quad (44)$$

$$x_2(k+1) = x_2(k) + 0.1\sin(x_3(k))x_4(k) + 0.1\cos(x_3(k))x_5(k) \quad (45)$$

$$x_3(k+1) = x_3(k) + 0.1x_6(k) \quad (46)$$

$$1.0852x_4(k+1) = -0.0039x_1(k) + (1.0765 + \Delta_{a44}(k))x_4(k) + (0.1 + \Delta_{b41}(k))u_1(k) + 0.01w(k) \quad (47)$$

$$\begin{aligned} 2.0575x_5(k+1) - 0.4087x_6(k+1) = & -0.0027x_2(k) + (2.0499 + \Delta_{a55}(k))x_5(k) \\ & - 0.4238x_6(k) + (0.1 + \Delta_{b52}(k))u_2(k) + 0.01w(k) \end{aligned} \quad (48)$$

$$\begin{aligned} -0.4087x_5(k+1) + 0.2153x_6(k+1) = & -0.4102x_5(k) + (0.2150 + \Delta_{a66}(k))x_6(k) \\ & + (0.1 + \Delta_{b63}(k))u_3(k) + 0.01w(k) \end{aligned} \quad (49)$$

$$y_1(k) = x_3(k) + w(k) \quad (50)$$

where $x_1(k)$, $x_2(k)$ and $x_3(k)$ are the X position, Y position and yaw angle on earth-fixed coordinate, $x_4(k)$, $x_5(k)$ and $x_6(k)$ are the ship body-fixed coordinate-based surge motion, sway motion and yaw angular velocity, $u_1(k)$, $u_2(k)$ and $u_3(k)$ are the control force and moment provided by the thrusters, the detailed modeling process for (44)–(50) can be found in [44].

Remark 4. The uncertain factors are considered for the nonlinear ship steering system (44)–(50) as $\Delta_{a44}(k) = 0.1085\sin(k)$, $\Delta_{a55}(k) = 0.2058\sin(k)$, $\Delta_{a66}(k) = 0.0215\sin(k)$, $\Delta_{b41}(k) = \Delta_{b52}(k) = \Delta_{b63}(k) = 0.01\sin(k)$, $\Delta_{e1}(k) = 0.1085\sin(k)$, $\Delta_{e2}(k) = 0.2058\sin(k)$ and $\Delta_{e3}(k) = 0.0215\sin(k)$. These factors may be caused by rust, corrosion, wear and tear, and the biofoulings adhering to the ship hull, which deteriorates the control performance. Moreover, the disturbance is considered to account for sea waves, currents, and winds generated by the external complex ocean environment. It should be noted that the effects of these factors on the X and Y position dynamics of the ship are relatively small. Therefore, the uncertainties and disturbances are incorporated into the velocity equations in (47)–(49).

In the research [48], the author presents a comprehensive discussion of the modeling and control problem of practical ship steering systems. Moreover, this type of mathematical model has been widely used in modeling practical ships. It is worth noting that the ship steering system (44)–(49) is also derived from [48]. Additionally, uncertainty and disturbance factors are included in this research, which are inevitable and more significant for ship steering systems.

Referring to [44], the operating range is considered within the control scenario of $x_3(k) \in [-90^\circ, 90^\circ]$. Accordingly, the T-SFDM of the nonlinear ship steering system and corresponding membership function are presented as follows:

$$\begin{cases} \sum_{\alpha=1}^3 \Phi_{\alpha} \{ \hat{\mathbf{T}}_{\alpha} x(k+1) \} = \sum_{\alpha=1}^3 \Phi_{\alpha} \{ \hat{\mathbf{A}}_{\alpha} x(k) + \hat{\mathbf{B}}_{\alpha} u(k) + \mathbf{W}_{\alpha} w(k) \} \\ y(k) = \sum_{\alpha=1}^3 \Phi_{\alpha} \{ \mathbf{C}_{\alpha} x(k) + \mathbf{V}_{\alpha} w(k) \} \end{cases} \tag{51}$$

where $x(k) = [x_1(k) \ x_2(k) \ x_3(k) \ x_4(k) \ x_5(k) \ x_6(k)]^T$, $u(k) = [u_1(k) \ u_2(k) \ u_3(k)]^T$, and the model matrices are presented as follows:

$$\mathfrak{T}_1 = \mathfrak{T}_2 = \mathfrak{T}_3 = \begin{bmatrix} 1 & 0 & 0 & 0 & 0 & 0 \\ 0 & 1 & 0 & 0 & 0 & 0 \\ 0 & 0 & 1 & 0 & 0 & 0 \\ 0 & 0 & 0 & 1.0852 & 0 & 0 \\ 0 & 0 & 0 & 0 & 2.0575 & -0.4087 \\ 0 & 0 & 0 & 0 & -0.4087 & 0.2153 \end{bmatrix},$$

$$\mathbf{A}_1 = \begin{bmatrix} 1 & 0 & 0 & 0.1 & -0.1\varepsilon_1 & 0 \\ 0 & 1 & 0 & 0.1\varepsilon_1 & 0.1 & 0 \\ 0 & 0 & 1 & 0 & 0 & 0.1 \\ -0.0039 & 0 & 0 & 1.0765 & 0 & 0 \\ 0 & -0.0027 & 0 & 0 & 2.0499 & -0.4238 \\ 0 & 0 & 0 & 0 & -0.4102 & 0.215 \end{bmatrix},$$

$$\mathbf{A}_2 = \begin{bmatrix} 1 & 0 & 0 & 0.1\varepsilon_2 & -0.1 & 0 \\ 0 & 1 & 0 & 0.1 & 0.1\varepsilon_2 & 0 \\ 0 & 0 & 1 & 0 & 0 & 0.1 \\ -0.0039 & 0 & 0 & 1.0765 & 0 & 0 \\ 0 & -0.0027 & 0 & 0 & 2.0499 & -0.4238 \\ 0 & 0 & 0 & 0 & -0.4102 & 0.215 \end{bmatrix},$$

$$\mathbf{A}_3 = \begin{bmatrix} 1 & 0 & 0 & 0.1\varepsilon_3 & 0.1 & 0 \\ 0 & 1 & 0 & -0.1 & 0.1\varepsilon_3 & 0 \\ 0 & 0 & 1 & 0 & 0 & 0.1 \\ -0.0039 & 0 & 0 & 1.0765 & 0 & 0 \\ 0 & -0.0027 & 0 & 0 & 2.0499 & -0.4238 \\ 0 & 0 & 0 & 0 & -0.4102 & 0.215 \end{bmatrix},$$

$$\mathbf{B}_1 = \mathbf{B}_2 = \mathbf{B}_3 = \begin{bmatrix} 0 & 0 & 0 \\ 0 & 0 & 0 \\ 0 & 0 & 0 \\ 0.1 & 0 & 0 \\ 0 & 0.1 & 0 \\ 0 & 0 & 0.1 \end{bmatrix}, \mathbf{C}_1 = \mathbf{C}_2 = \mathbf{C}_3 = [0 \ 0 \ 1 \ 0 \ 0 \ 0], \mathbf{V}_1 = \mathbf{V}_2 = \mathbf{V}_3 = 1 \text{ and}$$

$$\mathbf{W}_1 = \mathbf{W}_2 = \mathbf{W}_3 = \begin{bmatrix} 0 \\ 0 \\ 0 \\ 0.01 \\ 0.01 \\ 0.01 \end{bmatrix} \tag{52}$$

where $\varepsilon_1 = \sin(2^\circ)$, $\varepsilon_2 = \cos(88^\circ)$ and $\varepsilon_3 = \cos(-88^\circ)$. For the T-SFDM (51) and (52), the uncertainties are constructed with the following matrices:

$$\Delta_1(k) = \Delta_2(k) = \Delta_3(k) = \sin(k), \mathbf{H}_1 = \mathbf{H}_2 = \mathbf{H}_3 = \begin{bmatrix} 0 & 0 & 0 & 0 & 0 & 0 \\ 0 & 0 & 0 & 0 & 0 & 0 \\ 0 & 0 & 0 & 0 & 0 & 0 \\ 0 & 0 & 0 & 0.1 & 0 & 0 \\ 0 & 0 & 0 & 0 & 0.1 & 0 \\ 0 & 0 & 0 & 0 & 0 & 0.1 \end{bmatrix},$$

$$\mathbf{R}_{\mathfrak{I}1} = \mathbf{R}_{\mathfrak{I}2} = \mathbf{R}_{\mathfrak{I}3} = \begin{bmatrix} 0 & 0 & 0 & 0 & 0 & 0 \\ 0 & 0 & 0 & 0 & 0 & 0 \\ 0 & 0 & 0 & 0 & 0 & 0 \\ 0 & 0 & 0 & 1.0852 & 0 & 0 \\ 0 & 0 & 0 & 0 & 2.0575 & 0 \\ 0 & 0 & 0 & 0 & 0 & 0.2153 \end{bmatrix},$$

$$\mathbf{R}_{A1} = \mathbf{R}_{A2} = \mathbf{R}_{A3} = \begin{bmatrix} 0 & 0 & 0 & 0 & 0 & 0 \\ 0 & 0 & 0 & 0 & 0 & 0 \\ 0 & 0 & 0 & 0 & 0 & 0 \\ 0 & 0 & 0 & 1.0852 & 0 & 0 \\ 0 & 0 & 0 & 0 & 2.0575 & 0 \\ 0 & 0 & 0 & 0 & 0 & 0.2153 \end{bmatrix}, \mathbf{R}_{B1} = \mathbf{R}_{B2} = \mathbf{R}_{B3} = \begin{bmatrix} 0 & 0 & 0 \\ 0 & 0 & 0 \\ 0 & 0 & 0 \\ 0.1 & 0 & 0 \\ 0 & 0.1 & 0 \\ 0 & 0 & 0.1 \end{bmatrix} \tag{53}$$

Benefiting from the descriptor system representation, the T-SFDM (51)–(53) can also be utilized to describe the dynamic behaviors of a typical control system with the full-rank matrices $\mathbf{T}_1 = \mathbf{T}_2 = \mathbf{T}_3$. This advantage eliminates the need for additional transformation processes when constructing the mathematical

model for the ship steering system. Then, the triangular membership function is also designed in Fig. 6 for the T-SFDM (51)–(53) according to the operating points.

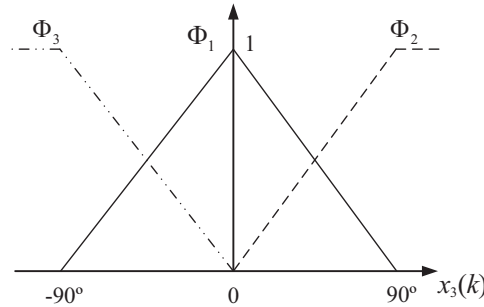


Figure 6: Membership function of the nonlinear ship steering system

Based on the T-SFDM (51)–(56) and Fig. 6, the following target model is also constructed for the nonlinear ship steering system (44)–(50).

$$\begin{cases} \sum_{\alpha=1}^3 \Phi_{\alpha} \left\{ \hat{\mathbf{T}}_{\alpha} x_d(k+1) \right\} = \sum_{\alpha=1}^3 \Phi_{\alpha} \left\{ \hat{\mathbf{A}}_{\alpha} x_d(k) \right\} \\ y_d(k) = \sum_{\alpha=1}^3 \Phi_{\alpha} \left\{ \mathbf{C}_{\alpha} x_d(k) \right\} \end{cases} \quad (54)$$

To demonstrate the P-D fuzzy tracking synthesis presented in Theorem 2, the tracking problem of time-varying trajectories is considered for ship steering control in this example. Moreover, the first-order hold is adopted to construct the target trajectories of $x_d(k)$ between different points. Selecting the parameter $\mu = 1$ and the initial condition $x(0) = [0 \ 0 \ 0 \ 0 \ 0 \ 0]^T$, the following gains are obtained by solving Theorem 2 using MATLAB and Algorithm 1.

$$\mathbf{T}_1^p = \begin{bmatrix} -0.0132 & -0.0004 & 0.0032 & -0.2782 & 0.0703 & -0.0001 \\ 0.0002 & -0.0587 & -0.0519 & 0.0074 & -0.4061 & 0.0218 \\ -0.0003 & -0.1024 & -0.1026 & 0.0527 & 0.8408 & 0.0408 \end{bmatrix},$$

$$\mathbf{T}_2^p = \begin{bmatrix} -0.0093 & 0.0014 & -0.0004 & -0.3992 & 0.2793 & -0.0001 \\ 0.0011 & -0.0455 & -0.0385 & -0.0167 & -0.6998 & 0.0167 \\ 0.0011 & -0.0782 & -0.0799 & 0.1239 & 0.7400 & 0.0314 \end{bmatrix},$$

$$\mathbf{T}_3^p = \begin{bmatrix} -0.0065 & 0.0005 & -0.0056 & -1.5966 & 0.1529 & 0.0002 \\ 0.0023 & -0.0366 & 0.0095 & 0.1065 & -2.4846 & 0.0118 \\ 0.0005 & -0.0553 & -0.0623 & 0.0845 & 0.8219 & 0.0231 \end{bmatrix},$$

$$\mathbf{T}_1^d = 10^4 \times \begin{bmatrix} 0.2643 & 0.0005 & -0.0001 & 0.8434 & 0.0020 & -0.00003 \\ 0.0004 & 0.2264 & 0.3003 & 0.0017 & 0.7365 & 0.0196 \\ 0.0008 & 0.3886 & 1.7370 & 0.0032 & 1.2640 & 0.1630 \end{bmatrix},$$

$$\mathbf{T}_2^d = 10^4 \times \begin{bmatrix} 0.2029 & 0.0003 & -0.0001 & 0.6476 & 0.0013 & -0.00001 \\ 0.0004 & 0.1741 & 0.2182 & 0.0014 & 0.5663 & 0.0137 \\ 0.0006 & 0.2985 & 1.3416 & 0.0024 & 0.9709 & 0.1259 \end{bmatrix},$$

$$\mathbf{T}_3^d = 10^3 \times \begin{bmatrix} 1.5053 & 0.0021 & -0.0006 & 4.8027 & 0.0093 & -0.0001 \\ 0.0023 & 1.2946 & 1.5290 & 0.0092 & 4.2087 & 0.0922 \\ 0.0045 & 2.2109 & 9.9910 & 0.0182 & 7.1925 & 0.9386 \end{bmatrix} \quad (55)$$

In order to better align with practical control scenarios for ship steering, the disturbance $w(k)$ is modeled as a random process in Fig. 7 to simulate the effects of ocean waves, winds, and currents, which persist over time.

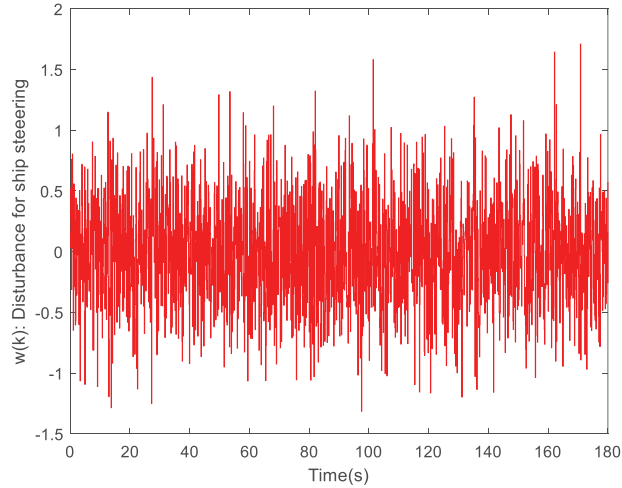


Figure 7: Disturbance of nonlinear ship steering system

Applying the P-D fuzzy tracking controller (6) with the gains in (55), the state responses of the nonlinear ship steering system (44)–(50) are obtained in Figs. 8–13.

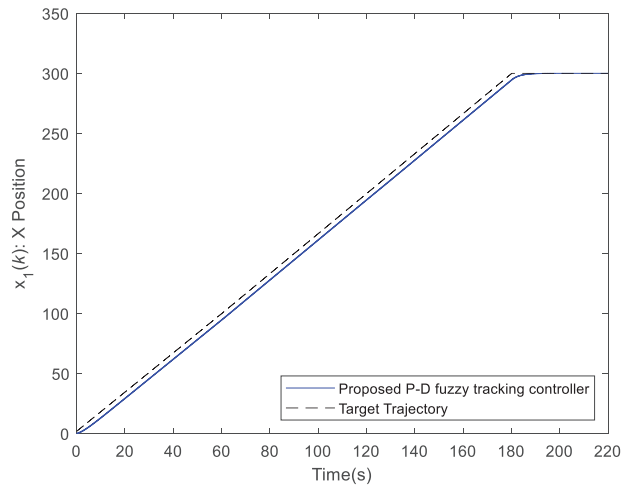


Figure 8: State $x_1(k)$ response of nonlinear ship steering system

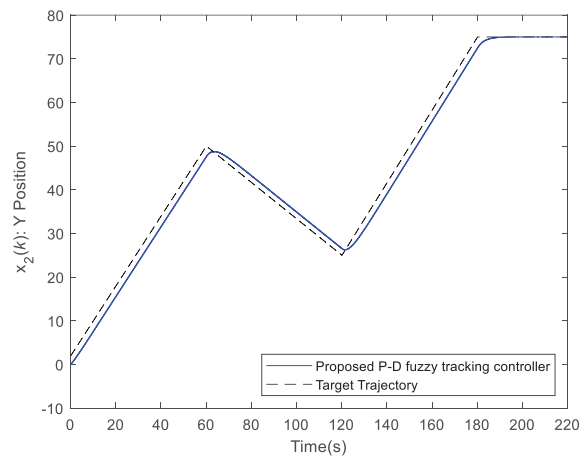


Figure 9: State $x_2(k)$ response of nonlinear ship steering system

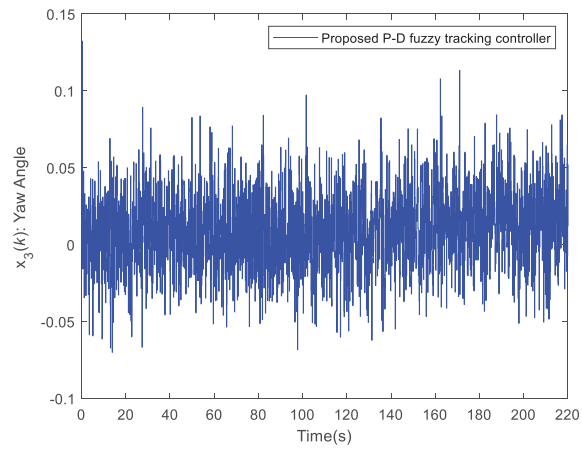


Figure 10: State $x_3(k)$ response of nonlinear ship steering system

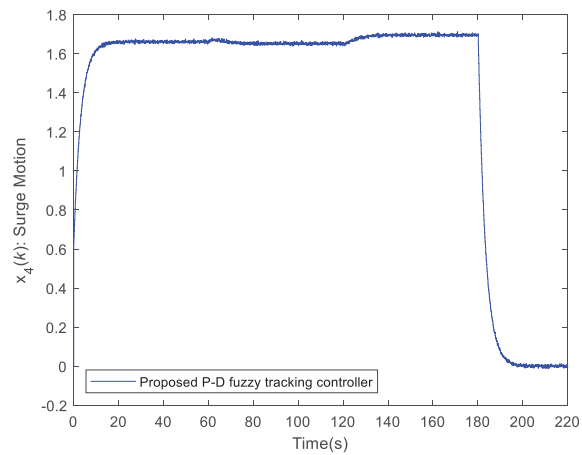


Figure 11: State $x_4(k)$ response of nonlinear ship steering system

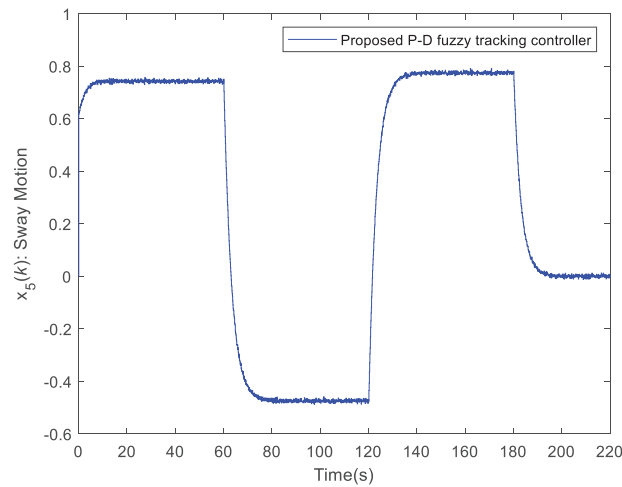


Figure 12: State $x_5(k)$ response of nonlinear ship steering system

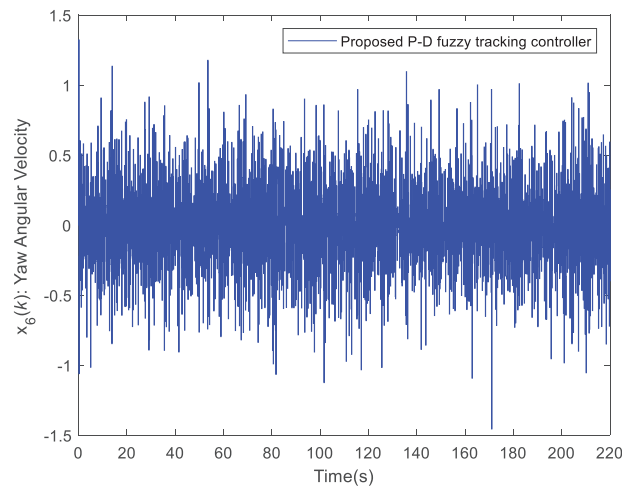


Figure 13: State $x_6(k)$ response of nonlinear ship steering system

In this simulation, the target trajectories for the X and Y positions of the ship are directly provided for the tracking purpose. Therefore, it is evident from Figs. 8 and 9 that the state responses of the ship can effectively track the desired trajectories. Ultimately, the ship reaches the designed destination. Figs. 11 and 12 also show that smooth surge and sway motions are achieved during the tracking process, even under the influence of uncertainties and disturbances. It is important to note that the magnitude of the disturbance $w(k)$ in Fig. 7, when applied to the state $x_6(k)$ is expressed in radians, so the effect of random disturbance is significantly more pronounced in Figs. 10 and 13.

To verify the disturbance dissipating ability of the ship steering system, the following calculation is given for the strictly input passive constraint (9) in Lemma 2.

$$\frac{\mu \sum_{k=1}^{220} w^T(k) w(k)}{2 \sum_{k=0}^{220} e_y^T(k) w(k)} = 0.05 < 1 \tag{56}$$

Thus, it is observed that the disturbance energy can be efficiently reduced in Figs. 11 and 12 when the passivity (55) is ensured. Finally, the minimized H₂ performance in Definition 2 is validated by the following calculation.

$$\left(\sum_{k=0}^{220} e_x^T(k) \Omega_e e_x(k) + u^T(k) \Omega_u u(k) = 16.4546 \right) < (\rho = 100) \tag{57}$$

Note that the minimized parameter in (57) is further larger than the value obtained in Example 1. This is due to the higher order of the ship steering system compared to the DC motor system. Additionally, a more complex random process is considered for the ship steering system. As the tracking performance must be guaranteed, the control effect cannot be minimized to an excessively small value.

Then, the MSE and MAE values are also provided as follows. Note that the main purpose is to directly track the X and Y positions in this simulation. Because of this reason, these performance indices are only presented for the first two states of ship steering systems (44)–(50). Based on the results in Figs. 8 and 9, the MSE and MAE values are calculated as follows:

$$\begin{aligned} Y_{MSE}^1 &= \frac{1}{220} \sum_{k=0}^{220} (x_1(k) - x_{1d}(k))^2 = 3.9549 \times 10^4, \\ Y_{MSE}^2 &= \frac{1}{220} \sum_{k=0}^{220} (x_2(k) - x_{2d}(k))^2 = 2.3182 \times 10^3, \\ Y_{MAE}^1 &= \frac{1}{220} \sum_{k=0}^{220} |x_1(k) - x_{1d}(k)| = 173.0075, \\ Y_{MAE}^2 &= \frac{1}{220} \sum_{k=0}^{220} |x_2(k) - x_{2d}(k)| = 43.5981 \end{aligned} \tag{58}$$

By comparing the MSE and MAE values in (58) with Table 1 of Example 1, it is observed that the values in this example are much larger. This is because the time-varying trajectory tracking problem is solved and tracking errors are inevitable, even though good tracking performance is achieved as shown in Figs. 8 and 9. To clearly demonstrate the tracking performance by using the proposed fuzzy tracking synthesis in Theorem 2, the ship trajectory and the target trajectory are provided in Fig. 14.

Based on Fig. 14, it is worth noting that the ship trajectory can still be well controlled to track the target trajectory under the influence of uncertainties and disturbances. It is concluded that the proposed P-D fuzzy tracking synthesis in Theorem 2 provides a more reasonable and applicable solution for practical control applications in nonlinear descriptor system form.

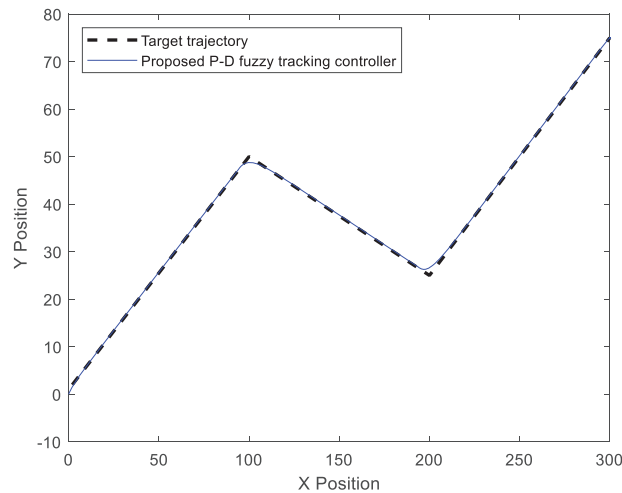


Figure 14: Trajectory of the nonlinear ship steering system

5 Conclusion

Based on the T-SFDM, a P-D fuzzy tracking synthesis is proposed for the nonlinear descriptor system in this research to ensure the tracking purpose while meeting multiple performance requirements. By representing the system in descriptor form, the proposed fuzzy tracking control approach can solve the control problems of both singular and typical systems. With the application of the PDC concept and P-D feedback technique, regularity and causality are ensured, and impulse behavior caused by the algebraic constraint is efficiently avoided. Considering the effects of uncertainties and disturbances, robust control and passive constraints are integrated into the fuzzy tracking controller design process. Moreover, the H_2 performance index, which evaluates the energy between states and control inputs in a minimized manner, is introduced to strike a better trade-off between the convergence rate and control effort, while preventing the control effort from growing too large. Based on the Lyapunov theory, the stability criteria are proposed to ensure asymptotic stability, robustness, and passivity, as well as minimize H_2 performance simultaneously, and the control problem is then reformulated as an LMI problem. The simulation presents the results of two examples, including a nonlinear DC motor system in singular form and a nonlinear ship steering system in typical form controlled by the proposed P-D fuzzy tracking synthesis. The simulation results validate that the proposed P-D fuzzy controller can achieve smoother state responses and preserve control forces while simultaneously ensuring the tracking purpose and satisfying multiple performance requirements. However, the fuzzy tracking synthesis design process still suffers from conservativeness, which prevents the H_2 performance and passivity constraint from reaching an ideal level. Further relaxation of the design process is worth investigating in future work.

Acknowledgement: Not applicable.

Funding Statement: This research was funded by the National Science and Technology Council (Taiwan) under contract NSTC113-2221-E-019-032.

Author Contributions: The authors confirm contribution to the paper as follows: Conceptualization, Yi-Chen Lee, Wen-Jer Chang and Yann-Horng Lin; methodology, Wen-Jer Chang, Yann-Horng Lin, Muhammad Shamrooz Aslam and Zi-Yao Lin; software, Wen-Jer Chang and Zi-Yao Lin; validation, Yi-Chen Lee, Yann-Horng Lin and Muhammad Shamrooz Aslam; formal analysis, Muhammad Shamrooz Aslam and Zi-Yao Lin; investigation, Yi-Chen Lee, Wen-Jer Chang and Yann-Horng Lin; resources, Muhammad Shamrooz Aslam and Zi-Yao Lin; data curation, Wen-Jer Chang,

Yann-Horng Lin and Zi-Yao Lin; writing—original draft preparation, Yi-Chen Lee and Yann-Horng Lin; writing—review and editing, Wen-Jer Chang and Muhammad Shamrooz Aslam; visualization, Zi-Yao Lin; supervision, Yi-Chen Lee and Wen-Jer Chang; project administration, Yi-Chen Lee and Wen-Jer Chang; funding acquisition, Wen-Jer Chang. All authors reviewed the results and approved the final version of the manuscript.

Availability of Data and Materials: Not applicable.

Ethics Approval: Not applicable.

Conflicts of Interest: The authors declare no conflicts of interest to report regarding the present study.

Abbreviations

T-SFM	Takagi-Sugeno Fuzzy Model
PDC	Parallel Distributed Compensation
P-D	Proportional-Difference
T-SFDM	Takagi-Sugeno Fuzzy Descriptor Model
T-SFDEM	Takagi-Sugeno Fuzzy Descriptor Error Model
LMI	Linear Matrix Inequality

References

1. Kumar R, Srivastava S, Gupta JRP. Comparative study of neural networks for control of nonlinear dynamical systems with lyapunov stability-based adaptive learning rates. *Arab J Sci Eng.* 2018;43(6):2971–93. doi:10.1007/s13369-017-3034-9.
2. Righi I, Aouaouda S, Chadli M, Khelil K. Robust controllers design for constrained nonlinear parameter varying descriptor systems. *Int J Robust Nonlinear Control.* 2021;31(17):8295–328. doi:10.1002/rnc.5415.
3. Luenberger D. Dynamic equations in descriptor form. *IEEE Trans Autom Control.* 1977;22(3):312–21. doi:10.1109/TAC.1977.1101502.
4. Tripathi M, Moysis L, Gupta MK, Fragulis GF, Volos C. Observer design for nonlinear descriptor systems: a survey on system nonlinearities. *Circuits Syst Signal Process.* 2024;43(5):2853–72. doi:10.1007/s00034-024-02617-1.
5. Li W, Du H, Feng Z, Ning D, Li W. Dynamic output-feedback event-triggered H_∞ control for singular active seat suspension systems with a human body model. *IET Control Theory Appl.* 2021;15(4):594–603. doi:10.1049/cth2.12064.
6. Lei M. Nonlinear diving stability and control for an AUV via singular perturbation. *Ocean Eng.* 2020;197(2):106824. doi:10.1016/j.oceaneng.2019.106824.
7. Susana Ramya L, Leelamani A. Resilient fuzzy control design of singular stochastic biological economic fishery model. *IET Control Theory Appl.* 2021;15(9):1214–29. doi:10.1049/cth2.12117.
8. Verghese G, Lévy B, Kailath T. A generalized state-space for singular systems. *IEEE Trans Autom Control.* 1981;26(4):811–31. doi:10.1109/TAC.1981.1102763.
9. Kumar A, Paitandi M, Gupta MK. Impulse eliminations for rectangular descriptor systems: a unified approach. *IEEE Control Syst Lett.* 2023;7(1):1357–62. doi:10.1109/LCSYS.2023.3240022.
10. Wang X, Zhong Z, Lam HK, Li Z. Reachable set bounding of output-feedback control for discrete-time large-scale IT-2 fuzzy descriptor systems using distributed event-based broadcasts. *Eng Appl Artif Intell.* 2021;100(2):104166. doi:10.1016/j.engappai.2021.104166.
11. Bunse-Gerstner A, Byers R, Mehrmann V, Nichols NK. Feedback design for regularizing descriptor systems. *Linear Algebra Appl.* 1999;299(1–3):119–51. doi:10.1016/S0024-3795(99)00167-6.
12. Zhuang G, Xia J, Sun W, Ma Q, Wang Z, Wang Y. Normalization and stabilization of neutral descriptor hybrid systems based on PD feedback control. *J Frankl Inst.* 2020;357(2):1070–89. doi:10.1016/j.jfranklin.2019.10.020.
13. Ren J, Li X, Mu Y. Proportional-difference observer design for singular systems in an LMI framework. *IEEE Access.* 2020;8:162449–57. doi:10.1109/ACCESS.2020.3021465.

14. Chang WJ, Su CL, Ku CC. Passive decentralized fuzzy control for Takagi-Sugeno fuzzy model based large-scale descriptor systems. *IEEE Access*. 2022;10(3):28656–69. doi:10.1109/ACCESS.2022.3158671.
15. Chang WJ, Lian KY, Su CL, Tsai MH. Multi-constrained fuzzy control for perturbed T-S fuzzy singular systems by proportional-plus-derivative state feedback method. *Int J Fuzzy Syst*. 2021;23(7):1972–85. doi:10.1007/s40815-021-01096-9.
16. Wu Q, Song Q, Zhao Z, Liu Y, Alsaadi FE. Stabilization of TS fuzzy fractional rectangular descriptor time-delay system. *Int J Syst Sci*. 2021;52(11):2268–82. doi:10.1080/00207721.2021.1882613.
17. Zhang X, Zhang L, Zhao X, Zhao N, Sharaf S. Real-time reachable set synthesis of Takagi-Sugeno fuzzy uncertain singular systems based on adaptive event-triggered scheme. *Int J Fuzzy Syst*. 2024;26(1):320–30. doi:10.1007/s40815-023-01599-7.
18. Lin TA, Lee YC, Chang WJ, Lin YH. Robust observer-based proportional derivative fuzzy control approach for discrete-time nonlinear descriptor systems with transient response requirements. *Processes*. 2024;12(3):540. doi:10.3390/pr12030540.
19. Montenegro D, Hernandez ME, Ramos GA. A realistic generator of power quality disturbances for practicing in courses of electrical engineering. *Comput Appl Eng Educ*. 2015;23(3):391–402. doi:10.1002/cae.21609.
20. Nguyen DN, Nguyen TA. Proposing a BSPID control strategy considering external disturbances for electric power steering (EPS) systems. *IEEE Access*. 2023;11:143230–49. doi:10.1109/ACCESS.2023.3343914.
21. Zheng Y, Tao J, Sun Q, Sun H, Chen Z, Sun M, et al. Soft Actor-Critic based active disturbance rejection path following control for unmanned surface vessel under wind and wave disturbances. *Ocean Eng*. 2022;247:110631. doi:10.1016/j.oceaneng.2022.110631.
22. Zhong Z, Wang X, Lam HK. Finite-time fuzzy sliding mode control for nonlinear descriptor systems. *IEEE/CAA J Autom Sin*. 2021;8(6):1141–52. doi:10.1109/JAS.2021.1004024.
23. Kukurowski N, Pazera M, Witczak M. Fault-tolerant tracking control for a descriptor system under an unknown input disturbances. *Electronics*. 2021;10(18):2247. doi:10.3390/electronics10182247.
24. Park JH. Further results on passivity analysis of delayed cellular neural networks. *Chaos Solit Fractals*. 2007;34(5):1546–51. doi:10.1016/j.chaos.2005.04.124.
25. Chang WJ, Ku CC, Huang PH. Robust fuzzy control for uncertain stochastic time-delay Takagi-Sugeno fuzzy models for achieving passivity. *Fuzzy Sets Syst*. 2010;161(15):2012–32. doi:10.1016/j.fss.2009.12.015.
26. Chang WJ, Lin YH, Lee YC, Ku CC. Investigating formation and containment problem for nonlinear multi-agent systems via interval type-2 fuzzy sliding mode tracking approach. *IEEE Trans Fuzzy Syst*. 2024;32(7):4163–77. doi:10.1109/TFUZZ.2024.3387045.
27. Lozano R, Brogliato B, Egeland O, Maschke B. *Dissipative systems analysis and control: theory and applications*. Berlin, Germany: Springer Science & Business Media; 2013.
28. Elsis M, Tran MQ, Hasanien HM, Turkey RA, Albalawi F, Ghoneim SS. Robust model predictive control paradigm for automatic voltage regulators against uncertainty based on optimization algorithms. *Mathematics*. 2021;9(22):2885. doi:10.3390/math9222885.
29. Hong YY, Apolinario GFD. Uncertainty in unit commitment in power systems: a review of models, methods, and applications. *Energies*. 2021;14(20):6658. doi:10.3390/en14206658.
30. Bardossy A, Duckstein L. *Fuzzy rule-based modeling with applications to geophysical, biological, and engineering systems*. London, UK: CRC Press; 2022.
31. Xu Y, Wang X, Liu M, Li N, Yu T. Fuzzy variable gain robust control of active magnetic bearings rigid rotor system. *IET Electr Power Appl*. 2024;18(1):90–106. doi:10.1049/elp2.12369.
32. Dass A, Srivastava S, Kumar R. A novel Lyapunov-stability-based recurrent-fuzzy system for the identification and adaptive control of nonlinear systems. *Appl Soft Comput J*. 2023;137(1):110161. doi:10.1016/j.asoc.2023.110161.
33. Wei Z, Ma Y. Robust H_∞ observer-based sliding mode control for uncertain Takagi-Sugeno fuzzy descriptor systems with unmeasurable premise variables and time-varying delay. *Inf Sci*. 2021;566(1):239–61. doi:10.1016/j.ins.2021.02.073.

34. Wang J, Zhuang G, Xia J, Chen G, Zhao J. Asynchronous dissipative control and robust exponential mean square stabilization for uncertain fuzzy neutral Markov jump systems. *J Syst Sci Complex*. 2022;35(4):1374–97. doi:10.1007/s11424-021-1005-4.
35. Chen X, Xu H, Feng M. H_2 performance analysis and H_2 distributed control design for systems interconnected over an arbitrary graph. *Syst Control Lett*. 2019;124:1–11. doi:10.1016/j.sysconle.2018.11.011.
36. Alsaade FW, Jahanshahi H, Yao Q, Al-zahrani MS, Alzahrani AS. A new neural network-based optimal mixed H_2/H_∞ control for a modified unmanned aerial vehicle subject to control input constraints. *Adv Space Res*. 2023;71(9):3631–43. doi:10.1016/j.asr.2022.02.012.
37. Kennouche A, Saifia D, Chadli M, Labiod S. Multi-objective H_2/H_∞ saturated non-PDC static output feedback control for path tracking of autonomous vehicle. *Trans Inst Meas Control*. 2022;44(11):2235–47. doi:10.1177/01423312221080461.
38. Nguyen AT, Dequidt A, Nguyen VA, Vermeiren L, Dambrine M. Fuzzy descriptor tracking control with guaranteed L_∞ error-bound for robot manipulators. *Trans Inst Meas Control*. 2021;43(6):1404–15. doi:10.1177/0142331220979262.
39. Nguyen HP, Bui NT. Tracking control based on Takagi-Sugeno fuzzy descriptor model for overhead crane combined with input shaping. *IEEE Access*. 2024;12:127507–21. doi:10.1109/ACCESS.2024.3456815.
40. Gao Z, Wang Z, Ji Z, Liu Y. Output strictly passive H_∞ control of discrete-time linear switched singular systems via proportional plus derivative state feedback. *Circuits Syst Signal Process*. 2020;39(8):3907–24. doi:10.1007/s00034-020-01353-6.
41. Gao Z, Liu Y, Wang Z. On stabilization of linear switched singular systems via PD state feedback. *IEEE Access*. 2020;8:97007–15. doi:10.1109/ACCESS.2020.2996687.
42. Chang WJ, Chang CM, Lin YH, Du J. Discrete-time robust fuzzy control synthesis for discretized and perturbed ship fin stabilizing systems subject to variance and pole location constraints. *J Mar Sci Technol*. 2021;26(1):201–15. doi:10.1007/s00773-020-00731-8.
43. Baranyi P, Korondi P, Patton RJ, Hashimoto H. Trade-off between approximation accuracy and complexity for TS fuzzy models. *Asian J Control*. 2004;6(1):21–33. doi:10.1111/j.1934-6093.2004.tb00181.x.
44. Lin ZY, Chang WJ, Aslam MS, Su CL, Lin YH. Difference state feedback fuzzy control of nonlinear discrete-time ship steering system in descriptor form. *Int J Fuzzy Syst*. 2024;1–22(3):299. doi:10.1007/s40815-024-01835-8.
45. Zhang L, Zong G, Zhao X, Zhao N, Sharaf S. Reachable set control for discrete-time Takagi-Sugeno fuzzy singular Markov jump system. *IEEE Trans Fuzzy Syst*. 2023;31(9):3173–84. doi:10.1109/TFUZZ.2023.3245634.
46. Shen H, Xing M, Wu ZG, Park JH. Fault-tolerant control for fuzzy switched singular systems with persistent dwell-time subject to actuator fault. *Fuzzy Sets Syst*. 2020;392(6):60–76. doi:10.1016/j.fss.2019.08.011.
47. Leonhard W. Control of electrical drives. Berlin, Germany: Springer Science & Business Media; 2001.
48. Fossen TI. Guidance and control of ocean vehicles. New York, NY, USA: Wiley; 1994.